Distinct Roles of Chromatin Insulator Proteins in Control of the *Drosophila* Bithorax Complex

Mikhail Savitsky,*,† Maria Kim,* Oksana Kravchuk,† and Yuri B. Schwartz*,1
*Department of Molecular Biology, Umeå University, 90187 Umeå, Sweden, and †Koltzov Institute of Developmental Biology, Russian Academy of Sciences, 119334 Moscow, Russia

ABSTRACT Chromatin insulators are remarkable regulatory elements that can bring distant genomic sites together and block unscheduled enhancer–promoter communications. Insulators act via associated insulator proteins of two classes: sequence-specific DNA binding factors and "bridging" proteins. The latter are required to mediate interactions between distant insulator elements. Chromatin insulators are critical for correct expression of complex loci; however, their mode of action is poorly understood. Here, we use the *Drosophila* bithorax complex as a model to investigate the roles of the bridging proteins Cp190 and Mod(mdg4). The bithorax complex consists of three evolutionarily conserved homeotic genes *Ubx*, *abd-A*, and *Abd-B*, which specify anterior–posterior identity of the last thoracic and all abdominal segments of the fly. Looking at effects of *CTCF*, *mod(mdg4)*, and *Cp190* mutations on expression of the bithorax complex genes, we provide the first functional evidence that Mod(mdg4) acts in concert with the DNA binding insulator protein CTCF. We find that Mod(mdg4) and Cp190 are not redundant and may have distinct functional properties. We, for the first time, demonstrate that Cp190 is critical for correct regulation of the bithorax complex and show that Cp190 is required at an exceptionally strong *Fub* insulator to partition the bithorax complex into two topological domains.

KEYWORDS HOX genes; chromatin; chromatin insulators; *Drosophila*; gene regulation

THE eukaryotic genome is folded extensively to fit inside the cell nucleus. The folding patterns vary between individual cells but certain conformations occur more frequently. In some cases, the likelihood of acquiring a particular conformation is linked to activation or repression of specific genes. Such links are especially important for complex loci in which multiple regulatory elements are positioned tens of thousands of base pairs (kb) away from their target promoters. The *Drosophila* bithorax complex is one of the best studied complex loci. The bithorax complex consists of three evolutionarily conserved homeotic genes *Ubx*, *abd-A*, and *Abd-B* that encode transcription factors and specify anterior–posterior identity of the last thoracic and all abdominal segments of the fly (Maeda and Karch 2006). Segment-specific expression of the bithorax complex genes is controlled by distal transcriptional enhancers and polycomb/trithorax response elements (PRE/TREs). The correct function of enhancers and PREs/TREs is further orchestrated by chromatin insulator elements that modulate the topology of the bithorax complex by mechanisms that are not well understood.

Chromatin insulator elements were first discovered in *Drosophila* and later found in vertebrates and plants. They are short (~1 kb) DNA elements that can block ("insulate") transcriptional activation of a promoter by a remote enhancer when interposed between the two. In contrast to transcriptional repression, insulation leaves the promoter transcriptionally competent so it is free to engage with other enhancers as long as those are not separated from the promoter by the insulator element.

The function of insulator elements depends on associated chromatin insulator proteins and here most of what we know comes from studies in *Drosophila*. Based on their biochemical and functional properties, the known *Drosophila* insulator proteins can be divided in three groups. The first group consists of nine sequence-specific DNA binding proteins: Su(Hw), CTCF, BEAF-32, Ibf1, Ibf2, Pita, ZIPIC (also known as CG7928), Dwg (also known as Zw5), and GAF (the product of *Trithorax-like* gene) (Geyer and Corces 1992; Zhao *et al.* 1995; Gaszner *et al.* 1999; Schweinsberg *et al.* 2004;

doi: 10.1534/genetics.115.179309
Manuscript received June 11, 2015; accepted for publication December 22, 2015; published Early Online December 23, 2015.
Supporting information is available online at www.genetics.org/lookup/suppl/doi:10.1534/genetics.115.179309/-/DC1.
[1]Corresponding author: Department of Molecular Biology, Umeå University, 90187 Umeå, Sweden. E-mail: yuri.schwartz@umu.se

Moon *et al.* 2005; Cuartero *et al.* 2014; Maksimenko *et al.* 2015; Wolle *et al.* 2015). The second group includes Cp190 and multiple protein isoforms encoded by the *mod(mdg4)* gene (Dorn *et al.* 2001; Pai *et al.* 2004; Van Bortle *et al.* 2012). The Cp190 and Mod(mdg4) proteins have no sequence specificity and may not be able to bind DNA directly. They can, however, mediate homotypic and heterotypic protein–protein interactions via their BTB/POZ (**B**road complex, **T**ramtrack, **B**ric-a-brac)/(**Po**xvirus and **Z**inc finger) domains. The third group includes biochemically diverse proteins: Elba1, Elba2, Elba3, and Shep (Aoki *et al.* 2012; Matzat *et al.* 2012). Though not required for enhancer blocking, these proteins appear to modulate the enhancer-blocking ability of insulator elements in a tissue- or stage-specific manner. Of all *Drosophila* insulator proteins, only CTCF has a clear ortholog in mammals (Baniahmad *et al.* 1990; Lobanenkov *et al.* 1990). Multiple lines of evidence indicate that insulator proteins act as multisubunit complexes (Matzat and Lei 2014). In addition, genomic mapping shows that insulator proteins bind chromatin in distinct combinations (Negre *et al.* 2010; Schwartz *et al.* 2012; Cuartero *et al.* 2014; Maksimenko *et al.* 2015). Importantly, only certain combinations of insulator proteins make these elements capable of blocking enhancer–promoter communications, suggesting that these proteins have additional unrelated functions.

Mechanisms by which insulator elements block enhancer–promoter communications are not yet clear. The most popular hypothesis suggests that insulator elements interact with each other and form chromatin loops that compete with chromatin looping involved in enhancer–promoter communication. Supporting this notion, certain insulator protein binding sites are enriched at bases of chromatin loops detected by genome-wide chromatin conformation capture (Hi-C) analysis (Rao *et al.* 2014). In this view, sequence-specific DNA binding insulator proteins of the first group serve to recruit proteins of the second group, which, via protein–protein interactions, "bridge" two or more insulator elements together. In *Drosophila*, Cp190 and Mod(mdg4) may be responsible for the "bridging" function. Like interactions and loops between enhancers and promoters, the interactions between insulator elements are likely transient and should be considered in probabilistic terms. Similarly, insulator interactions may bring different genomic elements together or juxtapose regulatory elements with appropriate target promoters (Gruzdeva *et al.* 2005; Ling *et al.* 2006; Splinter *et al.* 2006; Li *et al.* 2011).

Whether insulator elements are interchangeably used *in vivo* to both promote and block enhancer–promoter communicators or have a preference for either is an open question. An important step toward resolving this issue is to ask whether the two bridging proteins Cp190 and Mod(mdg4) are functionally different. Although both Cp190 and Mod(mdg4) have BTB/POZ domains, these domains differ in their amino acid sequences and their protein–protein interaction properties. Thus *in vitro* and in yeast two-hybrid assays, the BTB/POZ domains of Cp190 form homodimers (Bonchuk *et al.* 2011; Vogelmann *et al.* 2014) while the BTB/POZ domains of Mod(mdg4) form homo- and heterotypic multimers with the BTB/POZ domains of several other members of the *tramtrack* group (Golovnin *et al.* 2007; Bonchuk *et al.* 2011). Furthermore, the isolated BTB/POZ domains of Cp190 and Mod(mdg4) do not interact with each other (Bonchuk *et al.* 2011). The full-length Cp190 and the Mod(mdg4)67.2 protein isoform implicated in the function of the *gypsy* insulator element interact (Pai *et al.* 2004), presumably, via different domains.

Here, we use the *Drosophila* bithorax complex as a model to gain insight into the contribution of chromatin insulator proteins to regulation of complex loci and investigate the functions of *Drosophila* Cp190 and Mod(mdg4) proteins. We find that the key roles of the zygotic Cp190 and Mod(mdg4) proteins differ. The Mod(mdg4) proteins cooperate with sequence-specific DNA binding protein CTCF to promote expression of the *Abd-B* gene. In contrast, the Cp190 protein is critical for the function of an exceptionally strong insulator element that topologically separates the *Ubx* gene from posterior abdominal genes *abd-A* and *Abd-B*. This emphasizes the role of Cp190 as a central enhancer-blocking protein and points to potential preference of bridging insulator proteins toward blocking or facilitating enhancer–promoter communications.

Results

CTCF and Mod(mdg4) cooperate to enhance the Abd-B expression in the abdomen

Within the bithorax complex the CTCF, Cp190, and Mod(mdg4) proteins colocalize at multiple sites (Figure 1A) (Schwartz *et al.* 2012; Van Bortle *et al.* 2012) some of which can act as enhancer-blocking/boundary elements (Karch *et al.* 1994; Hagstrom *et al.* 1996; Zhou *et al.* 1996; Barges *et al.* 2000; Gruzdeva *et al.* 2005). Are all the three proteins involved in the bithorax complex regulation? If so, do they act redundantly, cooperate, or have distinct roles?

Of the three proteins, CTCF is the most studied, although reports do not always agree in details (Gerasimova *et al.* 2007; Mohan *et al.* 2007; Bonchuk *et al.* 2015). All studies conclude that loss of zygotic *CTCF* function results in posterior-to-anterior transformations of abdominal segments A8–A6, which is caused by the reduced expression of the *Abd-B* gene. However, they disagree as to whether zygotic CTCF is essential for viability. In line with observations from the Corces and Renkawitz laboratories (Gerasimova *et al.* 2007; Mohan *et al.* 2007), we find that flies carrying combinations of the loss-of-function alleles $CTCF^{y+1}/CTCF^{P35.2}$ or $CTCF^{P35.2}/CTCF^{9}$ (Figure 1B, Supporting Information, Figure S1, A and B) die as pharate adults. Both males and females show distinct posterior-to-anterior transformations of abdominal segments A8–A6 (Table1) when extracted from pupal cases. Consistently, we detect less Abd-B protein in the most posterior abdominal segments of larval ventral nerve cords (Figure 2, A and A′) and embryonic epidermises (Figure 2, C and C′) of the homozygous $CTCF^{y+1}$ mutants compared to corresponding

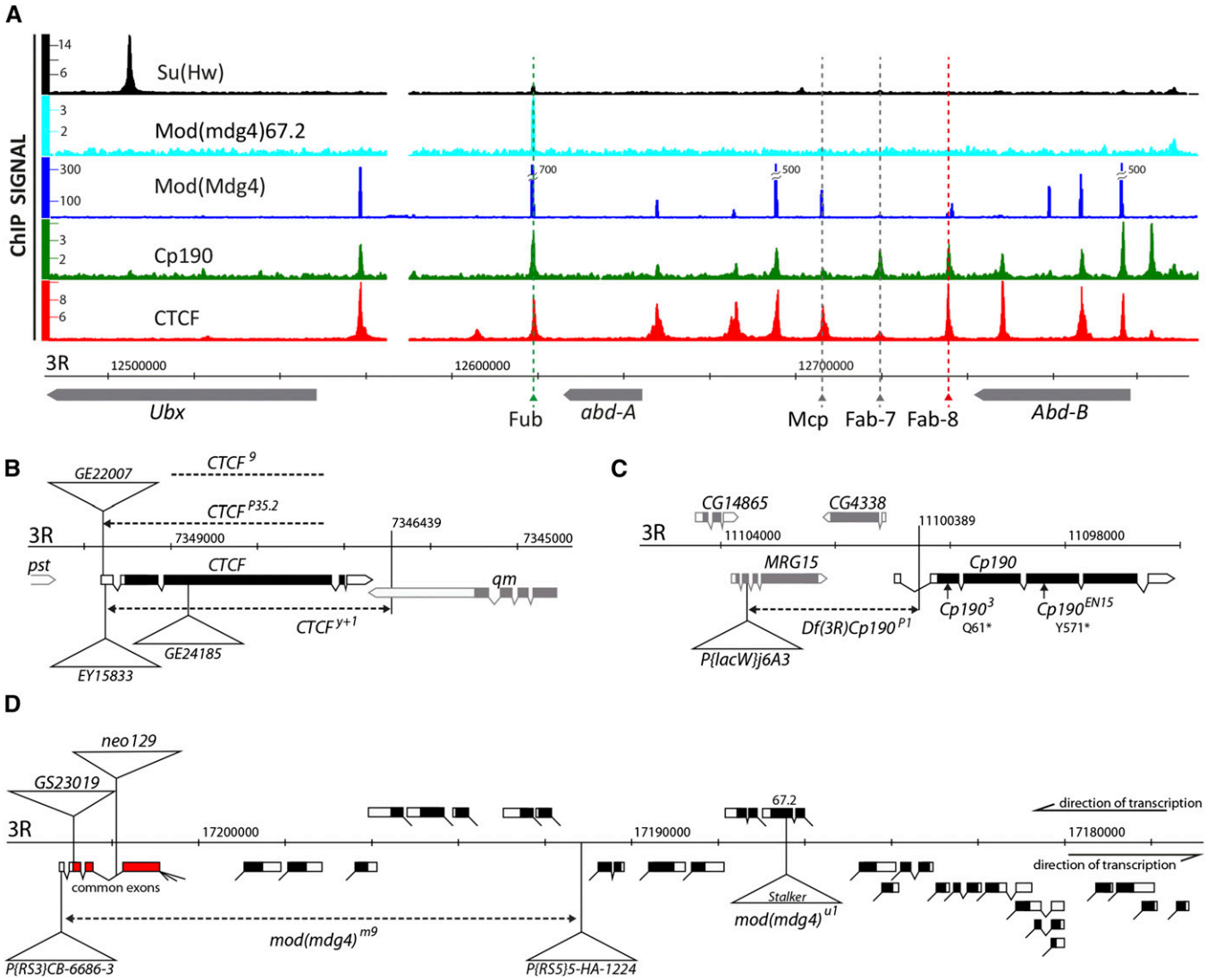

Figure 1 Overview of insulator protein binding to the bithorax complex and the alleles of the insulator protein genes. (A) Binding of insulator proteins to the bithorax complex in cultured *Drosophila* cells as defined by ChIP-chip [Su(Hw), Mod(mdg4)67.2, CTCF, Cp190 (Schwartz *et al.* 2012)] or ChIP-seq [Mod(mdg4) (Van Bortle *et al.* 2012)]. The ChIP signals (*y*-axes) are expressed as IP/INPUT ratios for all ChIP-chip experiments and as sequencing read density for Mod(mdg4) experiment. To accommodate full dynamic range of the Mod(mdg4) ChIP-seq signals the three highest peaks were trimmed and their top values indicated to the left. Positions of known enhancer-blocking/boundary elements are indicated by dashed lines. The three *HOX* genes of the complex (transcribed right to left) are shown below coordinate scale (Dm3, 2006 genome release). (B) Schematic representation of the molecular structure of *CTCF* alleles. Here and below positions of transposon insertions are marked with triangles and deletions are indicated with dashed lines. The insulator protein genes in B and C are transcribed from left to right. Arrowheads mark precisely mapped deletion breakpoints. (C) The structure of *Cp190* alleles. Vertical arrows mark the positions of the point mutations in $Cp190^{EN15}$ and $Cp190^{3}$ alleles. (D) Schematic representation of the *mod(mdg4)* gene and its alleles. The gene has four common 5′ exons (indicated in red) and a large number of alternatively spliced and *trans*-spliced 3′ exons located on both DNA strands (Dorn *et al.* 2001). Black boxes mark the coding parts of the exons and white boxes indicate the noncoding parts.

regions in flies with a copy of the wild-type *CTCF* gene. Flies homozygous for the $CTCF^{GE24185}$ allele (Figure 1B) or heterozygous for the combination of $CTCF^{y+1}/CTCF^{GE24185}$ alleles are viable but exhibit homeotic transformations similar to those seen in flies with the loss of *CTCF* function (Table 1, Figure 3). Recently, Bonchuk and coauthors proposed that $CTCF^{GE24185}$ is a null allele and argued that the lethality of other *CTCF* alleles is due to additional unrelated mutations (Bonchuk *et al.* 2015). It is hard to imagine that the three *CTCF* alleles ($CTCF^{y+1}$, $CTCF^{P35.2}$, and $CTCF^{9}$) all carry the same lethal mutation. Nevertheless, we asked whether the viability of flies with *trans*-heterozygous combinations of these alleles is "rescued" by supplying the CTCF protein from a transgene. For this, we fused the 2.6-kb open reading frame (ORF) of the *CTCF* gene (including two short introns) with the N-terminal One-STrEP-tag and placed the synthetic ORF under control of a strong *Ubi-p63E* promoter (Butcher *et al.* 2004). When integrated at 51C *attP* site by *phi*C31-mediated targeted recombination (Bischof *et al.* 2007) this *CTCF* transgene fully rescues the viability of the $CTCF^{y+1}/CTCF^{35.2}$ and

Table 1 Phenotypes of *CTCF*, *Cp190*, and *mod(mdg4)* mutants

Genotype	Phenotype description
mod(mdg4)^{m9}	Early pupal lethality (stages P1–P4).
mod(mdg4)^{neo129}	Early pupal lethality (stages P1–P4).
mod(mdg4)^{GS23019}	Reduced viability, males fertile, females sterile. Homeotic transformations: males, s6 with 4–5 bristles, t7 is slightly enlarged usually bears several bristles; females, s7 bears 8–14 (average 10) bristles, t8 occasionally bears a couple of small bristles.
mod(mdg4)^{GS23019}/mod(mdg4)^{m9}	Pharate adult lethality. Homeotic transformations: males, s6 has 3–5 bristles, t7 is enlarged and bears several bristles; females, s7 bears 7–14 (average 9.5) bristles often 3 large bristles instead of 2, t8 occasionally bears a couple of small bristles.
mod(mdg4)^{neo129}/mod(mdg4)^{m9}	∼75% early pupal lethality (stages P1–P4), ∼25% late pupa (stages P12–P15) to pharate adult lethality. Homeotic transformations: males, s6 with 3–7 (average 5) bristles, t7 is enlarged and bears several bristles; females, s7 bears 9–11 bristles occasionally 3 large bristles instead of 2, bristles on s7 occasionally lose orientation, t8 occasionally bears 1–2 bristles.
CTCF^{EY15833}[a]	Viable. Ten percent males and 20% females have wild-type appearance. Homeotic transformations: males, s6 with 0–4 bristles, t7 with 1 to several bristles (70%), enlarged t7 with a row of bristles (20%); females, s7 bears 8–16 (average 13) bristles, occasionally 3 large bristles instead of 2, occasionally (<5%) s7 shape is transformed toward s6 and bristles lose orientation, have small bristles on t8 (20%).
CTCF^{EY15833} mod(mdg4)^{u1}	Same as *CTCF^{EY15833}*.
CTCF^{EY15833} mod(mdg4)^{GS23019}	Viable, males fertile, females have reduced fertility. Homeotic transformations: males, genitalia rotated by 90–180°(100%), s6 with 4–15 (average 8) bristles, t7 is well developed, t8 is separated from t9 and bears 0–2 bristles; females, s7 with 10–15 (average 13) bristles, t8 always has a row of bristles.
CTCF^{y+1}/CTCF^{EY15833}	Viable. Homeotic transformations: males, s6 with 0–6 (average 2.5) bristles, 15% have genitalia rotated by ∼30°, t7 is well developed (100% penetrance); females, s7 with 9–14 (average 12) bristles, shape of s7 transformed toward s6 and bristles lose orientation (100%), have row of small (100%) and several large (15%) bristles on t8.
CTCF^{y+1} mod(mdg4)^{GS23019}/CTCF^{EY15833} mod(mdg4)^{m9}	Early pupal lethality (stages P1–P4), rare escapers die at pharate adult stage. Homeotic transformations: males, genitalia rotated by 180°, s6 has 4–11 (average 9) bristles, display small cuticle structure with 1–2 bristles that we interpret as s7 (designated as s7? in Figure 5C), t7 is well developed, t8 well separated from t9 and bears rows of large bristles; females, as *CTCF^{y+1}/CTCF^{EY15833}*, but t8 always has rows of large bristles.
CTCF^{y+1} mod(mdg4)^{neo129}/CTCF^{EY15833} mod(mdg4)^{m9}	Early pupal lethality (stages P1–P4).
CTCF^{GE24185}[b]	In addition to published description. Males, s6 has 3–13 (average 8) bristles; females, s7 with 8–15 (average 12) bristles, often display a bunch of small bristles on t8 (0–17 bristles, average 8).
CTCF^{y+1}/CTCF^{GE24185}	Viable. Homeotic transformations: males, genitalia rotated by 30–180° (70% penetrance), s6 with 4–9 (average 7) bristles, t7 is well developed; females, s7 with 8–12 (average 10) bristles, shape of s7 transformed toward s6 and bristles lose orientation, have row of large bristles on t8.
CTCF^{y+1}/CTCF$^{35.2}$	Pharate adult lethality. Homeotic transformations: males, genitalia rotated 90–180° (100%), s6 with 6–10 (average 8) bristles; females, s7 has 11–14 (average 12) bristles, shape of s7 transformed toward s6 and bristles lose orientation, have rows of large bristles on t8.
CTCF^{9}/CTCF$^{35.2}$	Pharate adult lethality. Rare escapers eclose but die within 24–48 hr. Homeotic transformations: males, genitalia rotated by 20–180° (90%), s6 with 4–8 (average 6) bristles; females, s7 with 12–16 (average 14) bristles, shape of s7 transformed toward s6 and bristles lose orientation, have rows of large bristles on t8.

(continued)

Table 1, *continued*

Genotype	Phenotype description
Cp190^{P1}/Cp190^{3}	Pharate adult lethality with rare (2%) escapers. Homeotic transformations: held out wings in escapers often blistered, the shape of t1 changed toward t2, t1 bears long bristles, inner support sclerite is absent or rudimentary. s1 is often visible but shows no bristles.
Cp190^{3}/Cp190^{EN15}	Same as *Cp190^{P1}/Cp190^{3}*.
CP190^{EN15}/CP190^{P1}	Same as *CP190^{P1}/CP190^{3}*, the escapers are slightly more frequent (5%), s1 usually shows bristles.
CTCF^{GE24185} Cp190^{EN15}/CTCF^{GE24185} Cp190^{P1}	Pharate adult lethality with rare (2%) escapers. Escapers are weak with partially unfolded wings, not able to move and feed. Homeotic transformations: A1 transformation is less pronounced compared to *Cp190^{EN15}/Cp190^{P1}*. The shape of t1 changes toward t2; however, large bristles are rare, s1 usually shows no bristles. The bristles on t1 are distributed more uniformly compared to wild type. Males, s6 has 0–4 (average 1) bristles, in 50% of males the t7 is not enlarged, in the other 50%, t7 is enlarged but often developed from only one side, t8 is well separated from t9 and usually visible as two bubble-like structures with a bunch of large bristles, genitalia rotated by 90–180° (100%); females, s7 with 5–11 (average 8) bristles, shape of s7 is transformed toward s6 and bristles lose orientation, t8 always has 7–19 (average 13) large bristles, which often form two rows.
Cp190^{P1} mod(mdg4)^{m9}/Cp190^{3} mod(mdg4) ^{GS23019}	Pupal lethality (stages P5–P7). The head and leg structures start to develop but no thorax and abdominal structures are visible.

[a] Reported as lacking homeotic transformations in Mohan *et al.* (2007).
[b] Described in detail in Mohan *et al.* (2007).

CTCF^{9}/CTCF^{y+1} flies. Moreover, after chromosomes of the original *CTCF^{y+1}* and *CTCF^{9}* stocks were allowed to recombine to remove associated lethal mutations, our transgene also rescues the viability of the homozygous *CTCF^{y+1}* and *CTCF^{9}* flies. Taken together, our results uphold the conclusion that zygotic *CTCF* function is essential for viability and indicate that *CTCF^{GE24185}* is not a null allele but a strong hypomorph.

A clean loss-of-function allele of the *mod(mdg4)* gene has not been described. However, flies with a strong hypomorphic *mod(mdg4)* mutation on a sensitized genetic background with reduced expression of the *Abd-B* gene were reported to have transformations of abdominal segment A5 to A4 (Dorn *et al.* 1993; Buchner *et al.* 2000). This suggests that Mod(mdg4) promotes *Abd-B* expression in a way that is different from CTCF. To investigate this issue further, we generated a clean null allele of the *mod(mdg4)* gene. For this, we induced recombination between the FRT sites of the two *P*-element transposons P[RS5]mod(mdg4)$^{5\text{-HA-}1224}$ and P[RS3]mod(mdg4)$^{CB\text{-}6686\text{-}3}$ (Golic and Golic 1996; Ryder *et al.* 2004) and obtained the 12-kb deletion (3R: 17191075–17203088) that removes the transcription start site, four exons common for all transcriptional isoforms, and eight downstream exons included in some of the transcripts (Figure 1D, Figure S1C). We dubbed this allele *mod(mdg4)^{m9}*. Flies homozygous for the *mod(mdg4)^{m9}* allele die during metamorphosis and produce no adult structures to examine possible homeotic transformations (Table 1). However, flies heterozygous for the combination of *mod(mdg4)^{m9}* with the strong hypomorphic allele *mod(mdg4)^{neo129}* (Figure 1D) (Dorn *et al.* 1993; Buchner *et al.* 2000) or with the weak hypomorphic allele *mod(mdg4)^{GS29013}* (Figure 1D, Figure S1D) survive longer and die as pharate adults. Flies homozygous for hypomorphic allele *mod(mdg4)^{GS29013}* (Figure 1D, Figure S1D) survive until the adult stage but have reduced viability and fitness. Careful examination of *mod(mdg4)^{GS29013}*, *mod(mdg4)^{m9}/mod(mdg4)^{GS29013}*, and *mod(mdg4)^{neo129}/mod(mdg4)^{m9}* flies shows that all have distinct posterior-to-anterior transformations

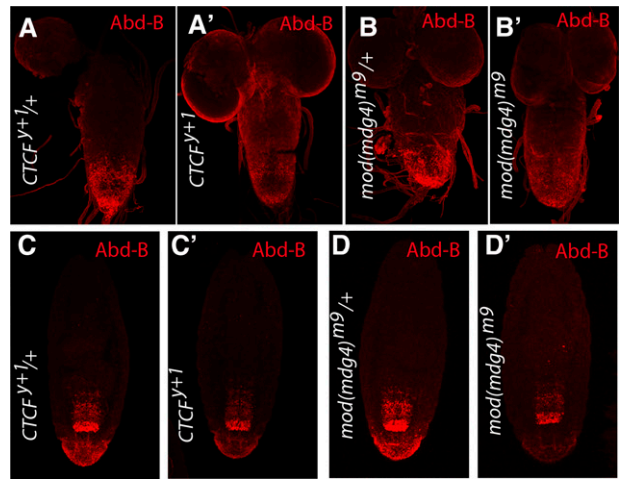

Figure 2 Loss of CTCF and Mod(mdg4) leads to reduction of the Abd-B levels in posterior segments of the larval nerve cord and embryonic epidermis. Ventral nerve cords from third instar larvae (A, A′, B, B′) and stage 17 embryos (C, C′, D, D′) of the indicated genotypes were immunostained with antibodies against Abd-B. Representative images show that in the mutants the Abd-B level in the most posterior segments of the nerve cords and embryonic epidermis is lower than in the matching heterozygous controls.

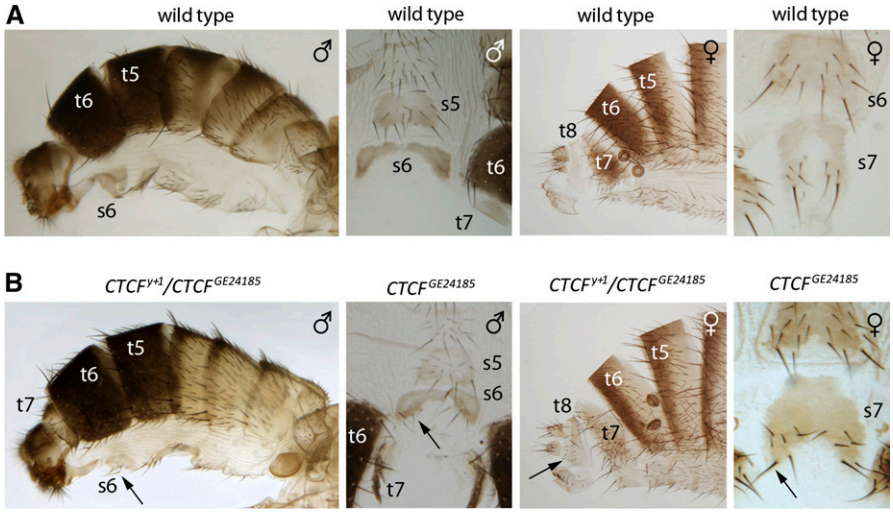

Figure 3 Homeotic transformations in *CTCF* mutant flies. Comparison of the cuticles from wild-type (A) and *CTCF* mutant flies (B) shows posterior-to-anterior transformations of abdominal segments A8–A6. The most obvious sign is the enlarged tergite of the seventh segment (t7) in *CTCF* mutant males. In wild-type males, t7 is essentially invisible. Also note additional bristles on the sternites of the sixth (s6) and seventh (s7) segments and on the tergite of the eighth segment (t8) that appear in the mutants but are absent in wild-type files (marked with arrows). We see no effect of *CTCF* mutations on morphology of the segments anterior to A6.

of abdominal segments A6–A8 (Figure 4). In agreement with these observations, we detect less Abd-B protein in posterior abdominal segments of the larval ventral nerve cord (Figure 2, B and B′) and embryonic epidermis (Figure 2, D and D′) of the homozygous *mod(mdg4)^{m9}* mutants compared with animals that have a copy of the wild-type *mod(mdg4)* allele. We note that flies homozygous for *mod(mdg4)^{u1}* allele, which disrupts exclusively the expression of the Mod(mdg4)67.2 protein isoform involved in the activity of *gypsy* and *gypsy*-like insulators (Georgiev and Gerasimova 1989; Georgiev and Kozycina 1996), display no homeotic transformations. This suggests that isoforms other than Mod(mdg4)67.2 are important to control posterior segment identity. Overall, we conclude that, like CTCF, some isoforms of the Mod(mdg4) protein promote *Abd-B* expression in the posterior abdominal segments.

Do CTCF and Mod(mdg4) cooperate to upregulate the *Abd-B* gene? To address this question, we compared homeotic transformations of single *CTCF* and *mod(mdg4)* mutants with those seen when the corresponding mutations are combined. Flies homozygous for the weak hypomorphic allele *CTCF^{EY15833}* (Table 1, Figure 1B) are viable and with 85% penetrance show weak transformation of segments A7 and A6 toward more anterior segments A6 and A5 (Table 1, Figure 5, A and B). Weaker transformations in the same direction are also seen in the hypomorphic allele *mod(mdg4)^{GS29013}* (Table 1, Figure 1D, and Figure 5, A and B). The *mod(mdg4)^{GS29013}* transformations are easiest to see in males whose A7 tergite (t7, Figure 5A) gets larger and the A6 sternite (s6, Figure 5A) acquires bristles that are normally absent. Strikingly, the double combination of the *CTCF* and *mod(mdg4)* alleles yields much stronger posterior-to-anterior transformations (Figure 5, A and B, Table 1). For instance, in *CTCF^{EY15833} mod(mdg4)^{GS29013}* males, transformation of the A7 tergite (t7) and rotation of genitalia are as strong as that of flies that carry strong *CTCF* mutations but, in addition, the tergite of abdominal segment A8 (t8) is partially transformed into t7 (Figure 5A). Combinations of weak and strong *CTCF* and *mod(mdg4)* alleles produce strong transformations that are not seen in flies homozygous for any of the individual mutant alleles (Figure 5C, Figure S2). For example, in such mutant males, the A8 tergite (t8) becomes separated from the tergite of segment A9 (t9). It is also bigger and has a row of bristles (Figure 5C). Enhanced homeotic transformations of the double mutants are specific and are not caused by changes in general genetic background. Thus, flies that have both the *CTCF^{EY15833}* allele and the *mod(mdg4)^{u1}* allele that affects exclusively the expression of Mod(mdg4)67.2 isoform, show transformations identical to those of the single *CTCF^{EY15833}* mutants (Table 1). Taken together, our observations suggest that CTCF and Mod(mdg4) act together to promote *Abd-B* expression.

Loss of CP190 leads to homeotic transformations different from those of CTCF and mod(mdg4) mutants

Homeotic phenotypes of *Cp190* mutants have not been described. To investigate this issue, we examined flies that were heterozygous for combinations of the two *Cp190* null alleles, *Cp190^{3}* and *Cp190^{P1}*, and a strong hypomorphic allele, *Cp190^{EN15}* (Figure 1C). The *Cp190^{3}* allele corresponds to a single nucleotide substitution that leads to a premature stop codon at position Q61 (Oliver *et al.* 2010). The *Cp190^{P1}* allele is a deletion of the promoter and the first exon of the *Cp190* transcription unit (Pai *et al.* 2004). The *Cp190^{EN15}* allele is a single nucleotide substitution that leads to a premature stop codon at position Y571 (Oliver *et al.* 2010). The majority of the *Cp190^{3}/Cp190^{P1}*, *Cp190^{3}/Cp190^{EN15}*, *Cp190^{P1}/Cp190^{EN15}* flies die as pharate adults. There are, however, a few that escape and die shortly after hatching. Strikingly, none of the above mutants display posterior-to-anterior transformations of abdominal segments A6–A8 that are characteristic of the *CTCF* and *mod(mdg4)* mutations. Instead, they show distinct transformation of abdominal segment A1 into A2. The tergite of the first abdominal segment changes the shape to that of segment A2 and displays long bristles normally present on the second abdominal tergite but

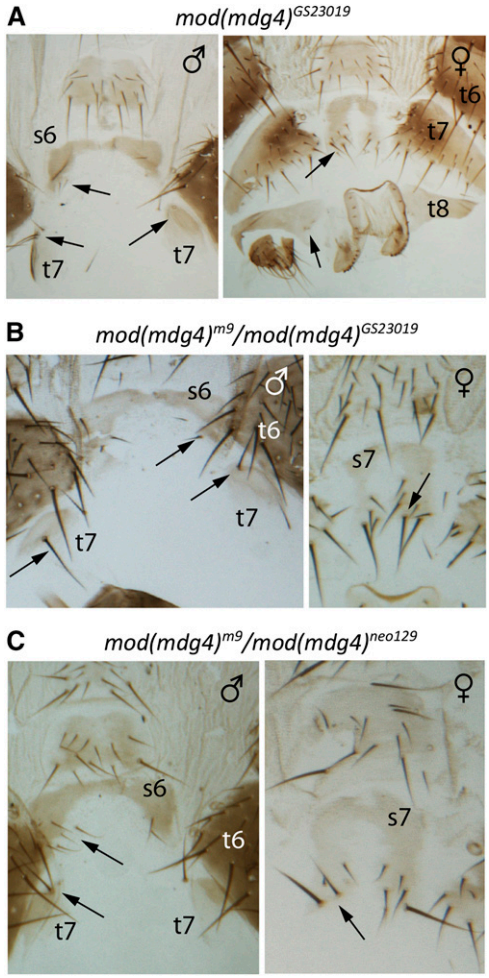

Figure 4 Mutations in the *mod(mdg4)* gene lead to homeotic transformations of posterior abdominal segments. Note that the number of additional bristles on t6, s6, and t7 (indicated with arrows) is greater in more severe allelic combinations: (A) the weakest allele, (B) intermediate combination, and (C) the strongest combination.

absent on the first (Figure 6A, Table 1). Additionally, the sternite of segment A1 acquires bristles characteristic of segment A2 (Figure 6A, Table 1). The identity of the A1 segment is defined by high *Ubx* gene expression and lack of *abd-A* gene expression. In contrast the A2 segment is defined by high expression of *abd-A* (Karch *et al.* 1990; Macias *et al.* 1990; Singh and Mishra 2014). Therefore, the transformation of segment A1 toward A2 in the *Cp190* mutants suggests that in these flies the *abd-A* gene is erroneously expressed in segment A1. Indeed, when we compare the immunostaining of epithelia from wild-type and $Cp190^{3}/Cp190^{P1}$ pupae we see that the latter have patches of cells within the first abdominal segment (A1) that stain with antibodies against Abd-A (Figure 6, B and C, Figure S3). Abd-A is known to directly repress the *Ubx* gene (Struhl and White 1985; Macias *et al.* 1990). Consistently, we see that patches of A1 cells that show ectopic *abd-A* expression in the $Cp190^{3}/Cp190^{P1}$ mutants are also weakly stained with antibodies against the Ubx protein (Figure 6, B and C, Figure S3).

The homeotic phenotypes of the Cp190 mutants are due to the impaired function of the Fub insulator that separates the bithorax complex into two topological domains

Strikingly, the homeotic transformations of the *Cp190* mutants are very similar to those seen in flies with the *Fub* deficiency that removes 4.3 kb between the upstream regulatory regions of the *Ubx* and *abd-A* genes (Bender and Lucas 2013) (Figure 1). Bender and Lucas proposed that *Fub* removes a boundary element that prevents the activation of *abd-A* by the *bxd* enhancers of the *Ubx* gene that are active in segment A1. Taken together, these observations suggest that the Cp190 protein plays an important role in establishing this putative insulator/boundary element. In support of this, the DNA fragment removed by the *Fub* deletion spans the site cobound by Cp190, Mod(mdg4)67.2, Su(Hw), and CTCF in wild-type embryos and cultured cells (Negre *et al.* 2010; Schwartz *et al.* 2012).

To test this hypothesis, we first analyzed recently published a Hi-C map of chromosomal contacts within wild-type embryonic nuclei (Schuettengruber *et al.* 2014). Consistent with previous reports, we find that all three genes of the bithorax complex are contained within a broad topological domain that spans ~330 kb from the 3′ end of the *Ubx* gene to a region ~10 kb upstream of the *Abd-B* gene (Sexton *et al.* 2012). The Hi-C map also reveals that the topological domain of the bithorax complex is further split into two subdomains demarcated by the insulator protein binding site removed by the *Fub* deletion (Figure 7A). This supports the idea that the Cp190-dependent *Fub* element plays a critical role in separating *Ubx* and the abdominal genes. We then asked whether the putative *Fub* insulator element can block enhancer–promoter communications in a transgenic assay and whether this block requires Cp190. To this effect, we PCR amplified a 981-bp DNA fragment underneath the *Fub* site and inserted it as an FRT cassette between the promoter and the upstream wing and body enhancers of the reporter *yellow* gene (Figure S4). A functional insulator element is expected to block the upstream enhancers but have no impact on the activation of the *yellow* promoter by the downstream bristle enhancer (Geyer and Corces 1992). The resulted construct contained an *attB* site for *phi*C31-mediated targeted integration (Bischof *et al.* 2007) and *P*-element ends to test the enhancer-blocking ability in different chromosomal contexts after *P*-mediated mobilization (Spradling and Rubin 1982). An integration of the *Fub* transgenic construct in the 51D landing site (Figure S4) (Bischof *et al.* 2007) of flies lacking the endogenous *yellow* function yields adults with light colored body and wings but black bristles (Figure 7B). The FLP-mediated excision of the transgenic *Fub* fragment (*ΔFub*) restores the pigmentation of wings and body to that of wild-type flies (Figure 7B). We therefore conclude that *Fub* acts as a strong enhancer blocking element in the chromatin context of the landing site. To test the enhancer-blocking ability of *Fub* insulator in different chromosomal contexts, we mobilized the

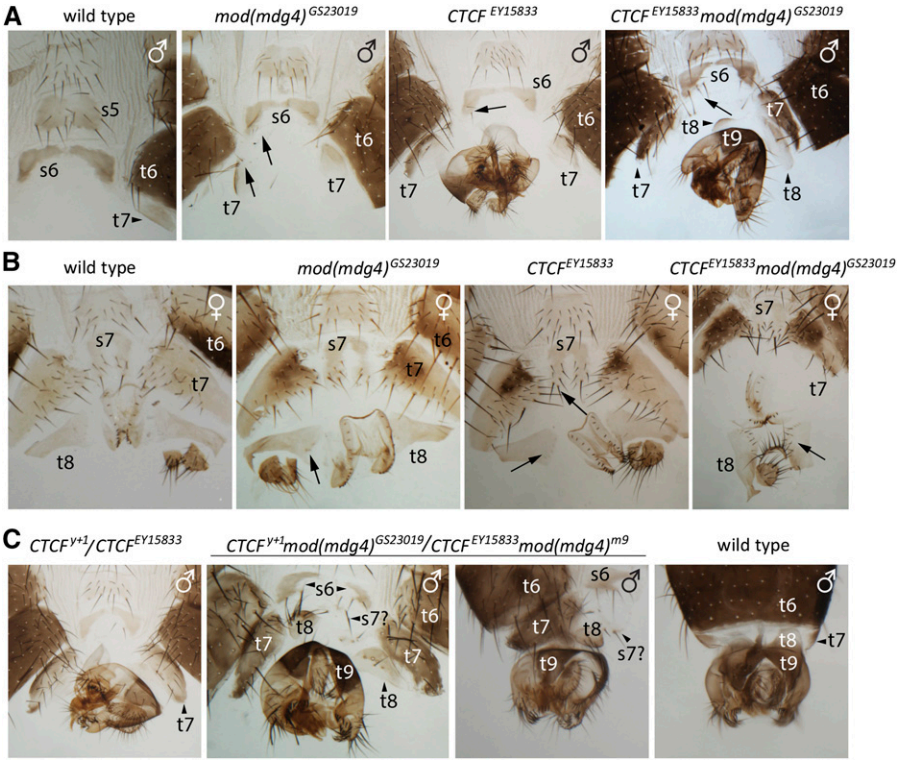

Figure 5 Genetic interactions between *CTCF* and *mod(mdg4)* mutations. Comparison of male (A) and female (B) flies with individual weak mutations in the *CTCF* and *mod(mdg4)* genes to flies with a combination of these alleles shows more pronounced homeotic transformations of posterior abdominal segments in flies carrying both mutations. Double combinations of weak [$CTCF^{EY15833}$ and $mod(mdg4)^{GS23019}$] and strong [$CTCF^{y+1}$ and $mod(mdg4)^{m9}$] alleles (C) produce extreme homeotic phenotype not seen in flies homozygous for any of the individual null alleles. Thus, in the $CTCF^{y+1}$ $mod(mdg4)^{GS23019}/CTCF^{EY15833}$ $mod(mdg4)^{m9}$ mutants, t8 becomes separated from t9 and also enlarges and gets a row of bristles. Positions of some tergites and sternites are indicated by arrowheads. Some of the additional bristles present in the mutants are marked with arrows.

transgene from the 51D landing site using *P*-element-mediated transposition and established 14 independent lines bearing transgenes at different loci. Of these lines, 13 lacked *yellow* expression in wings and body (Figure 8) and one showed some wing and body pigmentation. In this line, the pigmentation was weaker than in wild-type or *ΔFub* flies. These observations suggest that the enhancer blocking ability of *Fub* is robust and independent of the chromatin context. *Fub* appears to block enhancers as robustly as the paradigmatic *gypsy* insulator (Figure 8).

The introduction of the *Cp190* mutant background impairs the ability of *Fub* to block the upstream enhancers (Figure 7B). In contrast, loss of *CTCF* function causes only slight darkening of wings and body and we see no changes in the phenotype of transgenic flies carrying $mod(mdg4)^{GS23019}$, $mod(mdg4)^{u1}$ (lacking only Mod(mdg4)67.2 isoform, not shown) or a combination of $su(Hw)^{v}/su(Hw)^{f}$ mutations (Figure S5). We conclude that *Fub* is the unusually strong Cp190-dependent insulator element that separates the bithorax complex into two topologically independent domains and that the main phenotype of the zygotic loss of *Cp190* function is due to the impaired function of *Fub*.

Genetic interactions between Cp190 and CTCF

The binding profiles of Cp190, CTCF, and Mod(mdg4) within the bithorax complex are quite similar. Yet, the *Cp190* mutants show drastically different homeotic transformations compared to flies deficient for *CTCF* or *mod(mdg4)* functions. This could be due to functional differences between Cp190 and Mod(mdg4) proteins, partial redundancy of CTCF and other DNA binding proteins that recruit Cp190 and Mod(mdg4) to chromatin, the amounts and stability of maternally loaded Cp190 and Mod(mdg4), or a combination thereof. To get an insight in this complex issue, we looked at the phenotypes of flies that combine the *Cp190* mutations with mutations in *mod(mdg4)* or *CTCF*.

As a start, we recombined the $Cp190^{P1}$ mutation with $mod(mdg4)^{m9}$ and the $Cp190^{3}$ mutation with $mod(mdg4)^{GS23019}$. Although $Cp190^{P1}/Cp190^{3}$ and $mod(mdg4)^{m9}/mod(mdg4)^{GS23019}$ flies die as pharate adults with fully formed cuticles (Table 1), the $Cp190^{P1}$ $mod(mdg4)^{m9}/Cp190^{3}$ $mod(mdg4)^{GS23019}$ flies die as pupae prior to development of adult thorax and abdominal structures. Thus, we could not assess whether *Cp190* mutations enhance or suppress abdominal transformations of the *mod(mdg4)* mutants. In another attempt to answer this question, we compared the staining of the single $Cp190^{P1}/Cp190^{P1}$ and $mod(mdg4)^{m9}/mod(mdg4)^{m9}$ mutant embryos to the double $Cp190^{P1}$ $mod(mdg4)^{m9}/Cp190^{P1}$ $mod(mdg4)^{m9}$ mutants with antibodies against the Abd-B protein (Figure S6). Consistent with the lack of visible posterior abdominal transformations in the pharate adults, the immunostaining of $Cp190^{P1}/Cp190^{P1}$ embryos does not differ from that of the heterozygous control. The $mod(mdg4)^{m9}/mod(mdg4)^{m9}$ and the double $Cp190^{P1}$ $mod(mdg4)^{m9}/Cp190^{P1}$ $mod(mdg4)^{m9}$ mutant embryos both display weaker immunostaining of the posterior embryonic epidermis compared to the heterozygous control. However, we see no conclusive evidence that the presence of the $Cp190^{P1}$ mutation enhances or

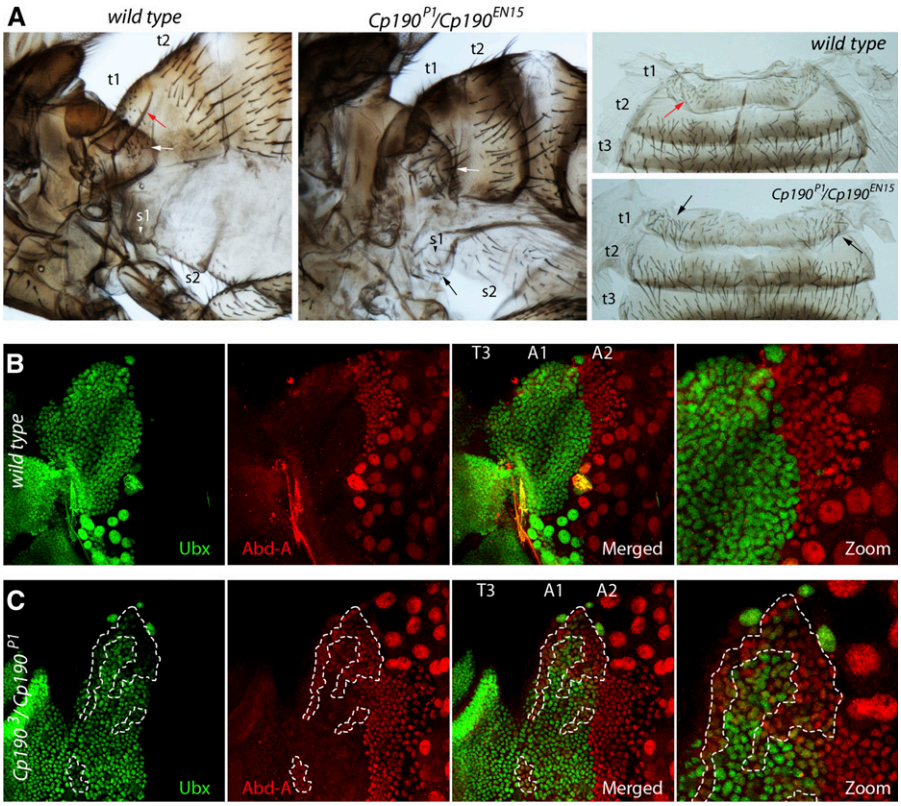

Figure 6 Loss of Cp190 function leads to ectopic expression of the *abd-A* gene in abdominal segment A1 and partial transformation of A1 toward A2. (A) Comparison of cuticles from wild-type and $Cp190^{P1}/Cp190^{EN15}$ flies shows that in the mutant flies the tergite of the first abdominal segment (t1) changes the shape to that of segment A2 and displays long bristles (black and white arrows) normally present on the second abdominal tergite (t2) but absent on t1. Similarly, the sternite of segment A1 (s1) acquires bristles characteristic of segment A2. The red arrow indicates the characteristic cuticle structure of the wild-type t1, which is absent in the Cp190 deficient flies. Immunostaining of epithelia from wild-type (B) and $Cp190^{3}/Cp190^{P1}$ (C) pupae indicates that loss of the *Cp190* function leads to ectopic coexpression of the *abd-A* and *Ubx* genes in some cells of segment A1. The pictures show corresponding parts of developing adult epithelia (small diploid cells) along with remnants of larval epithelia (large polyploid cells). In wild-type pupae the Abd-A- and Ubx-positive cells segregate along the boundary between segments A1 and A2. In the *Cp190* mutants, the A1 segment has patches of cells (marked with white dashed lines) that express Abd-A. Note that these Abd-A-positive cells also have lower Ubx expression. Individual cells are best seen in the blowup (zoom) of the upper right quarters of the merged images.

suppresses the reduction of *Abd-B* expression caused by $mod(mdg4)^{m9}$.

Next we examined homeotic transformations of the $CTCF^{GE24185}$ $Cp190^{EN15}/CTCF^{GE24185}$ $Cp190^{P1}$ mutants (Figure 9). In contrast to *mod(mdg4)* mutations that enhance posterior-to-anterior transformations of the sixth and seventh abdominal segments caused by the lack of *CTCF*, the *Cp190* mutations appear to suppress them. Thus in half of the $CTCF^{GE24185}$ $Cp190^{EN15}/CTCF^{GE24185}$ $Cp190^{P1}$ males the tergites of the seventh abdominal segment (t7) are of the same size as in wild-type flies and in the remaining half, t7 are much smaller compared to single *CTCF* mutants (Table 1, Figure 9, A and B). Similarly the sternites of the male A6 (s6) have very few bristles and the number of bristles in the female s7 is no longer as high as in single *CTCF* mutants (Table 1, Figure 9, A and B). Surprisingly, although *Cp190* mutations seem to suppress the transformation of A6 and A7 caused by the *CTCF* deficiency, they appear to enhance the posterior-to-anterior transformation of A8. Thus, the $CTCF^{GE24185}$ $Cp190^{EN15}/CTCF^{GE24185}$ $Cp190^{P1}$ males have t8 separated from t9 (the two are normally fused and remain fused in the single *CTCF* mutants) and the $CTCF^{GE24185}$ $Cp190^{EN15}/CTCF^{GE24185}$ $Cp190^{P1}$ females display larger numbers of bristles on t8 compared to single *CTCF* mutants. In addition, we see genitalia rotated in 100% of the $CTCF^{GE24185}$ $Cp190^{EN15}/CTCF^{GE24185}$ $Cp190^{P1}$ males compared to 30% penetrance of this phenotype in $CTCF^{GE24185}$ mutants. Taken together, our observations suggest that, unlike Mod(mdg4), the Cp190 protein does not generally cooperate with CTCF in promoting the *Abd-B* expression. However, Cp190 may enhance the *Abd-B* expression specifically in A8 and A9, at least when the CTCF function is impaired.

Unexpectedly, we find that *CTCF* mutations partially suppress the transformation of segment A1 toward segment A2 caused by the *Cp190* deficiency. Although in the double $CTCF^{GE24185}$ $Cp190^{EN15}/CTCF^{GE24185}$ $Cp190^{P1}$ mutants the shape of the A1 tergite (t1) still changes toward t2 and the bristles become less dense compared to wild-type flies (Figure 9C), the t1 bristles do not elongate (compare Figure 9C and Figure 6A) and s1 does not acquire bristles (Table 1).

Fub is the unusual class 12 insulator element

Fub shows exceptionally robust enhancer blocking comparable to that of the paradigmatic *gypsy* insulator. We have previously grouped genomic sites cobinding Su(Hw), CTCF, Cp190, and Mod(mdg4) insulator proteins into so-called class 12 but their functional properties were not investigated (Schwartz *et al.* 2012). We therefore asked whether strong enhancer blocking is a property inherent to elements that cobind Su(Hw), CTCF, Cp190, and Mod(mdg4). To this end, we PCR amplified eight ~1-kb-long DNA fragments from different class 12 sites and subjected them to the same enhancer-blocking assays as the *Fub* insulator element. When integrated at the 51D landing site five of eight class 12 sites showed some degree of enhancer blocking. However, in all cases the block was less strong and showed greater variability

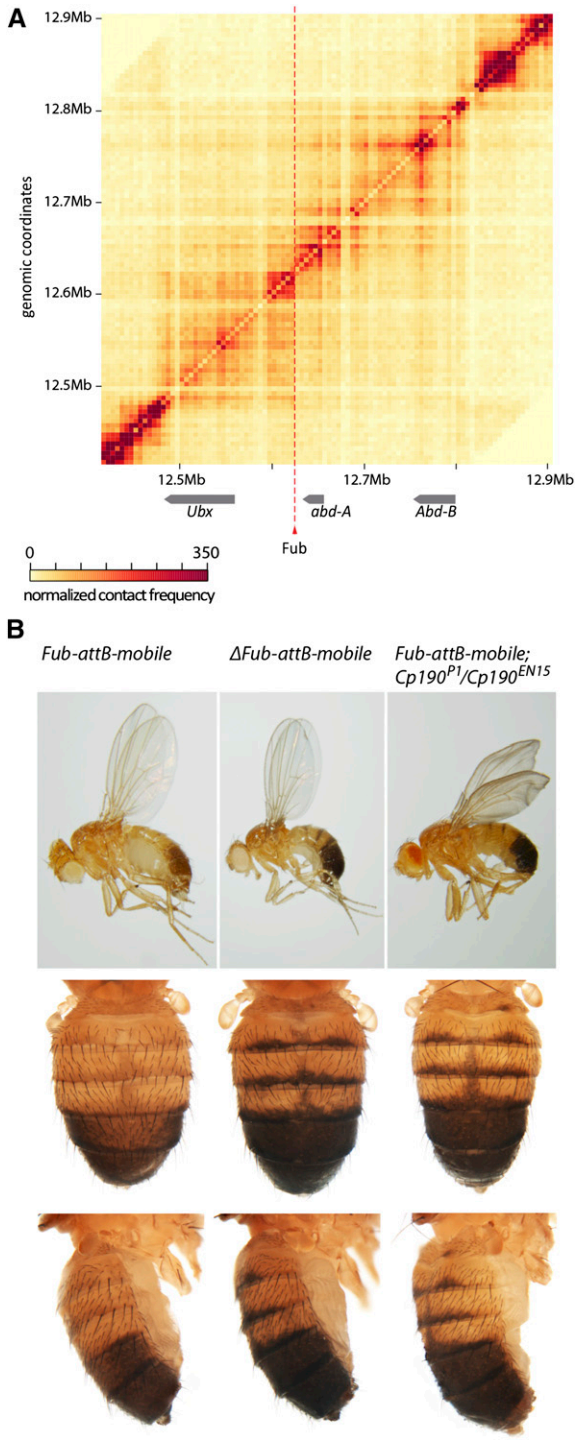

Figure 7 *Fub* is a topological boundary and a strong Cp190-dependent enhancer blocker. (A) The heat map of normalized contact frequencies (from Schuettengruber *et al.* 2014) within an ~500-kb stretch of chromosome 3R centered on the bithorax complex. The genes of the complex, transcribed from right to left, are shown underneath the *x*-coordinate axis. The coordinate scale is in Dm3, 2006 genome release. The position of the *Fub* insulator (dashed line) splits the topological domain of the bithorax complex into two subdomains. (B) *Fub* blocks interactions between upstream enhancers and the promoter of the *yellow* gene. Flies with the original *Fub-attB-mobile* insertion have black bristles and poorly pigmented abdomen and wing blades. However, when the *Fub* element is excised by FLP recombination (*ΔFub-attB-mobile*) or the mutant Cp190 background is introduced, the pigmentation of the abdomen and wing blades increases to nearly wild-type level.

when the transgenes were mobilized from the 51D landing site (Figure 8). This argues that the cobinding of Su(Hw), CTCF, Cp190, and Mod(mdg4) or other recently identified Cp190-interacting proteins (Pita, Ibf1, Ibf2, and ZIPIC) (Cuartero *et al.* 2014; Maksimenko *et al.* 2015) does not automatically predict a strong enhancer-blocking ability. It appears that *Fub* has additional features that make it an exceptionally strong insulator element.

Discussion

The *Drosophila* bithorax complex is a paradigmatic example of a homeotic selector locus that specifies anterior–posterior body axes. It is also an exemplary case of a multifaceted gene regulation that combines inputs from distal enhancers, noncoding RNAs, and epigenetic regulators and modulators of 3D chromatin topology. Here, we use the bithorax complex as a model to gain insight in the contribution of chromatin insulator proteins to regulation of complex loci and to gain insight into functional differences between the two bridging insulator proteins Cp190 and Mod(mdg4).

Mod(mdg4) promotes expression of the Abd-B gene

Until now, the functional role of the Mod(mdg4) proteins at insulator elements was limited to the specific Mod(mdg4)67.2 isoform that is implicated in enhancer blocking by the *gypsy* insulator (Georgiev and Gerasimova 1989; Gerasimova *et al.* 1995). It seems that the main function of Mod(mdg4)67.2 at the *gypsy* insulator is to prevent the associated Su(Hw) protein from acting as transcriptional repressor (Gerasimova *et al.* 1995; Georgiev and Kozycina 1996). Consistently, genomic sites that bind Su(Hw) protein in the absence of Mod(mdg4)67.2 act as repressive elements (Schwartz *et al.* 2012; Soshnev *et al.* 2013). *mod(mdg4)* is a complex gene that encodes ~30 protein isoforms through a *trans*-splicing of pre-mRNAs produced from both DNA strands (Dorn *et al.* 2001). All isoforms differ in their C-terminal regions and share the common N-terminal region of 402 amino acids that contains the BTB/POZ domain. Although mutations that disrupt the Mod(mdg4)67.2 protein isoform are viable, hypomorphic mutations that truncate Mod(mdg4) proteins within their common N-terminal part are lethal and have pleiotropic phenotypes that range from meiotic chromosome segregation defects in males (Soltani-Bejnood *et al.* 2007) to enhancement of the position effect variegation (Dorn *et al.* 1993; Buchner *et al.* 2000; Gause *et al.* 2001). Some of the lethal mutations were reported to affect expression of homeotic genes, although there is little agreement with regards to which genes are affected and to what extent. Thus, Dorn and colleagues described the changes in the pigmentation of the abdominal segment A5, suggesting that, in this segment, expression of

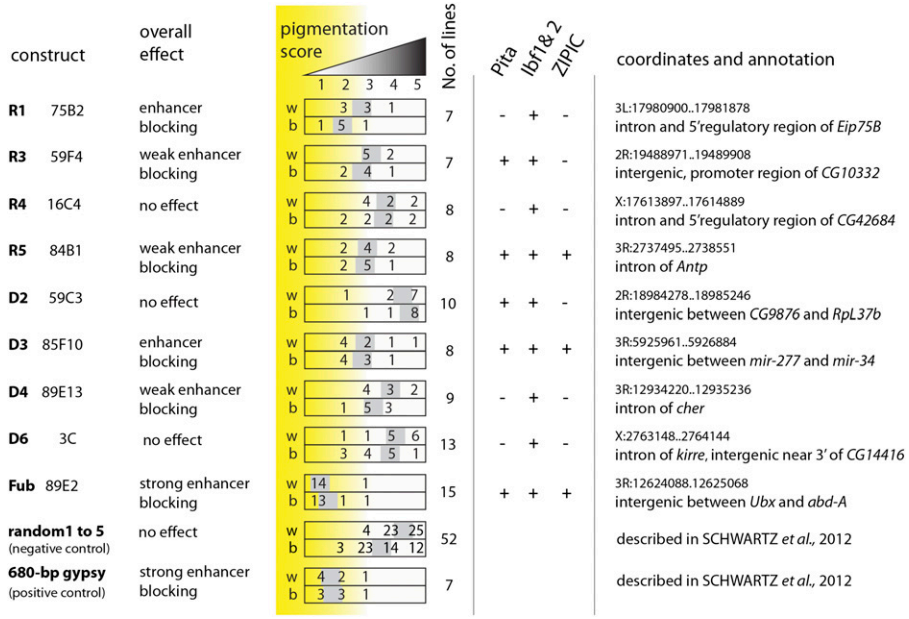

Figure 8 The results of *yellow* enhancer-blocking test. Transgenic constructs (the names of the constructs are shown in the leftmost column in boldface type and cytological locations of corresponding class 12 binding sites are indicated immediately to the right) were integrated at the 51D landing site and then mobilized to multiple genomic locations. Based on the average pigmentation score, each of the class 12 sites was ranked from having no effect to a strong enhancer blocker. The pigmentation of wings (w) and body (b) was scored on a 5-grade scale (illustrated as a triangle) with the score of 5 corresponding to wild-type pigmentation and the score of 1 corresponding to no pigmentation (Gruzdeva *et al.* 2005). Numbers in rectangles correspond to numbers of transgenic lines with corresponding pigmentation score. Shaded boxes indicate the "average" pigmentation score for each construct. An average score is often a fractional number and its position is displayed accordingly. The total number of independent transgenic lines examined is indicated to the right of the pigmentation score diagrams. The tested class 12 sites are annotated to indicate whether they also cobind Pita, Ibf1, Ibf2, or Zipic insulator proteins and to show their genomic coordinates and relation to the closest gene. Note, that from all tested sites, *Fub* is by far the strongest enhancer blocker that surpasses even the *gypsy* insulator (positive control). The negative control dataset was produced by combining published data from five different constructs carrying randomly selected DNA fragments that do not bind any known insulator proteins (Schwartz *et al.* 2012).

the *Abd-B* gene is reduced and that A5 is partially transformed into A4 (Dorn *et al.* 1993; Buchner *et al.* 2000). On the other hand, Gerasimova and Corces reported indiscriminate and complete loss of the bithorax complex gene expression (Gerasimova and Corces 1998), although they did not check for homeotic phenotypes. In both cases the effects of Mod(mdg4) loss were attributed to its role in counteracting repression of homeotic genes by Polycomb complexes (Dorn *et al.* 1993; Gerasimova and Corces 1998; Buchner *et al.* 2000).

Here, we carefully examined morphological phenotypes of flies with several combinations of mutant alleles of *mod(mdg4)*. We do not see any distinct changes in pigmentation of the A5 segment, although this cannot be completely excluded, and we see no transformations that are indicative of indiscriminate loss of the bithorax complex gene expression. Instead, we detect transformations of the most posterior abdominal segments toward their anterior counterparts, which are accompanied by reduction of the *Abd-B* expression. These transformations resemble defects seen in flies with impaired CTCF function. Because *mod(mdg4)* mutations enhance transformations caused by the *CTCF* deficiency and the CTCF and Mod(mdg4) proteins bind many of the same sites within the bithorax complex (Figure 1A) and genome-wide (Van Bortle *et al.* 2012), we favor the idea that the two act in concert as part of the same molecular pathway. This is, to our knowledge, the first functional evidence that CTCF and Mod(mdg4) act together and it would be very interesting to test, in the future, whether genomic sites cobound by the two proteins outside the bithorax complex behave in a similar way.

What is the mechanism by which Mod(mdg4) and CTCF promote expression of *Abd-B*? The answer is likely to be complex. Mammalian CTCF protein promotes long-range interactions between regulatory elements (Ong and Corces 2014) and chromatin conformation capture (3C) assays suggest that many sites within the bithorax complex engage in long-distance *trans*-interactions (Cleard *et al.* 2006; Lanzuolo *et al.* 2007; Schuettengruber *et al.* 2014). The *Abd-B* expression is regulated by a set of segment-specific regulatory modules that consist of transcriptional enhancers, an epigenetic maintenance element (PRE/TRE), and an adjacent insulator element that is often bound by Mod(mdg4) and/or CTCF. These insulator elements may promote the interaction of the corresponding enhancers with the *Abd-B* promoter and Mod(mdg4) and CTCF may be part of this process. Since Mod(mdg4) and CTCF bind in the vicinity of some of the *Abd-B* transcription start sites, they may also promote transcription more directly.

The role of CTCF and Mod(mdg4) at the bithorax complex likely involves more than just upregulation of *Abd-B* in posterior abdominal segments. Deletion of individual insulator elements from the *Abd-B* regulatory region cause segment-specific anterior-to-posterior transformations (Galloni *et al.* 1993; Mihaly *et al.* 1997; Barges *et al.* 2000; Iampietro *et al.* 2008). This indicates that the insulators prevent more potent enhancers that activate *Abd-B* in more posterior segments from acting in the adjacent anterior segments. We do not reliably detect anterior-to-posterior transformations in any of our *CTCF* and *mod(mdg4)* mutants. However, Mohan *et al.* (2007) reported A4-to-A5 transformations caused by *CTCF* mutations. Why are the gain-of-function transformations less obvious compared to the *Abd-B* loss-of-function phenotypes? It is possible that CTCF and Mod(mdg4) are simply not required for blocking the posterior enhancers from

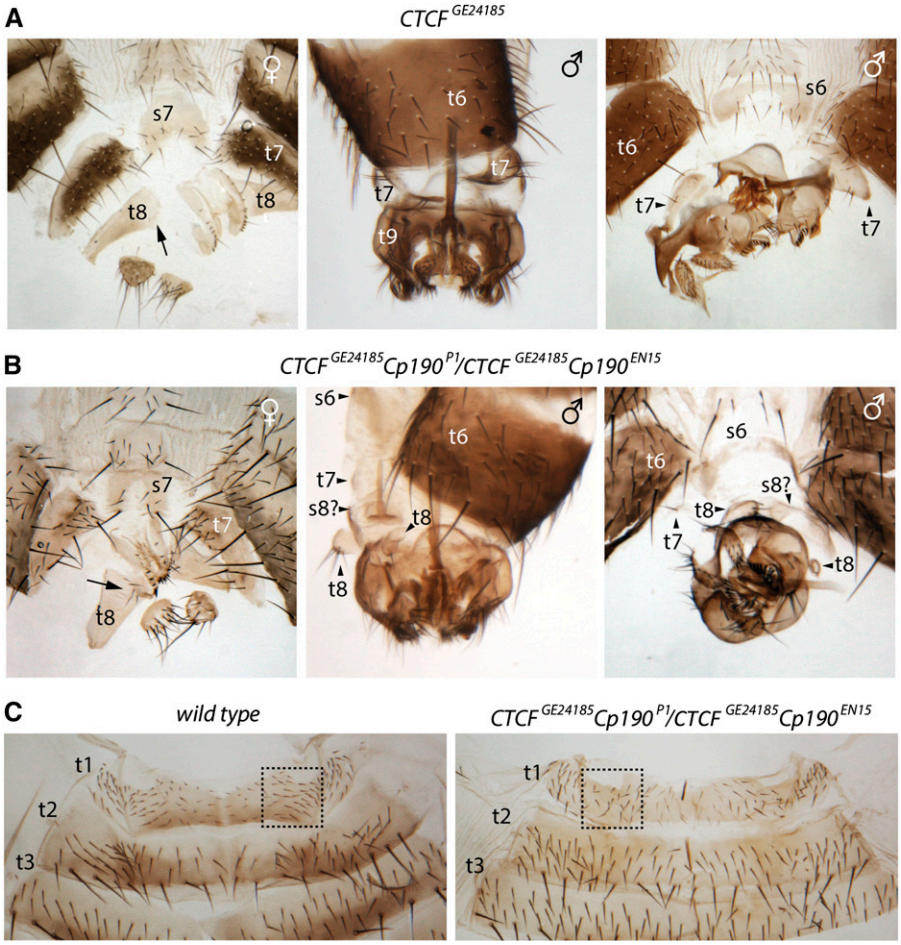

Figure 9 Genetic interactions between the *Cp190* and *CTCF* mutations. Cuticles of the $CTCF^{GE24185}/CTCF^{GE24185}$ (A) and $CTCF^{GE24185}$ $Cp190^{EN15}/CTCF^{GE24185}$ $Cp190^{P1}$ (B) females and males are compared side by side. The t7, enlarged in the *CTCF* mutant males, appears normal in males deficient for both *CTCF* and *Cp190*. The double mutant males also lack bristles on s6. At the same time, A8 of the *CTCF* and *Cp190* double mutants shows much stronger posterior-to-anterior transformation. The double mutant males have t8 separated from t9 and females have larger numbers of bristles on t8. Note also a strong rotation of genitalia in the double mutant males. (C) *CTCF* mutation partially suppresses A1-to-A2 transformation caused by Cp190 mutations. In the *CTCF* and *Cp190* double mutants, the shape of t1 changes toward that of t2 and bristles become less dense compared to wild-type flies (marked with dashed rectangle). However, the t1 bristles do not elongate (compare to Figure 6A) and s1 does not acquire bristles (not shown).

activating *Abd-B* in the more anterior segments. However, as pointed out by François Karch, the interpretation is likely more complex (Karch 2015). On one hand, the Abd-B protein is required to produce the gain-of-function phenotypes. On the other hand, the *CTCF* and *mod(mdg4)* mutants have reduced *Abd-B* expression and hence may produce too little Abd-B to manifest the anterior-to-posterior transformations.

The role of Cp190 in control of the bithorax complex

Current models often group the Cp190 and Mod(mdg4) proteins as functionally similar factors required to mediate interactions between distant insulator elements (Van Bortle and Corces 2012; Matzat and Lei 2014; Le Gall *et al.* 2015). Consistently, they bind many of the same sites within the bithorax complex (Figure 1A). We were, therefore, surprised to find that zygotic loss of Cp190 and Mod(mdg4) affects the bithorax complex in very different ways. While Mod(mdg4) promotes expression of the *Abd-B* gene in posterior abdominal segments, the Cp190 protein is critical to prevent erroneous expression of the *abd-A* gene anterior to its normal expression domain. To the best of our knowledge, this is the first evidence of the role of Cp190 in regulation of homeotic genes. Transformations of *CP190* mutants are strikingly similar to those of flies with the deletion of the *Fub* insulator element (Bender and Lucas 2013). This argues that the phenotype of the *Cp190* mutants is due to compromised *Fub* function. Consistently, we show that the ability of *Fub* to block enhancer–promoter communication in transgenic assays requires Cp190. Overall, this and earlier genome-wide studies (Negre *et al.* 2011; Schwartz *et al.* 2012), highlight the critical role of Cp190 in blocking unwanted enhancer–promoter interactions.

Our interpretations are limited by the fact that Cp190 is maternally loaded to the embryo. Nevertheless, the maternal contribution does not easily explain why the loss of zygotic Cp190 suppresses the A7-to-A6 and A6-to-A5 transformations caused by *CTCF* mutations while the loss of Mod(mdg4) enhances them. Together with previously documented biochemical differences (Bonchuk *et al.* 2011), our observations suggest that Cp190 and Mod(mdg4) are functionally distinct. It is tempting to speculate that Cp190 may be "specialized" in blocking long-range chromatin interactions while Mod(mdg4) may be tailored to promote enhancer–promoter communications.

Fub is an exceptionally strong chromatin insulator

The Cp190-dependent *Fub* insulator element is unusual in its exceptionally robust enhancer blocking ability, which is on par with that of the prototypic *gypsy* insulator element from the 5′ region of the eponymous retrotransposon (Geyer and

Corces 1992) and the strongest native *gypsy*-like *62D* insulator element described by Pamela Geyer and colleagues (Parnell *et al.* 2006; Kuhn-Parnell *et al.* 2008). As far as we know, *Fub* and *62D* are the strongest insulator elements naturally present in the *Drosophila* genome (Figure 8) (Golovnin *et al.* 2003; Parnell *et al.* 2003; Gruzdeva *et al.* 2005; Parnell *et al.* 2006; Ramos *et al.* 2006; Rodin *et al.* 2007; Schwartz *et al.* 2012). The strength of the *gypsy* insulator is explained by its unusual composition of an array of 12 binding sites for the Su(Hw) protein (Spana *et al.* 1988). What makes *62D* and *Fub* very strong insulators is not yet clear. Our transgenic tests suggest that, in the case of *Fub*, it is not simply the cobinding of Su(Hw), CTCF, CP190, Mod(mdg4), Ibf1/2, Pita, and ZIPIC, since other insulator protein binding sites of this kind block enhancer–promoter communication in variable and generally weaker fashion. Comparative analysis of multiple strong endogenous insulator elements is needed to reveal what makes a robust insulator. The feature that sets the *Fub* element apart is its residence at the boundary between topological domains. We speculate that screening for boundaries of topological domains that cobind multiple insulator proteins may help to identify additional strong endogenous insulator elements and ultimately understand their mechanics.

Methods

Enhancer blocking test constructs

DNA fragments representing *Fub* and the other class 12 insulator protein binding sites: Fub, 3R: 12624088-12625068; R1, 3L: 17980900-17981878; R3, 2R: 19488971-19489908; R4, X: 17613897-17614889; R5, 3R: 2737495-2738551; d2, 2R: 18984278-18985246; d3, 3R: 5925961-5926884; d4, 3R: 12934220-12935236; and d6, X: 2763148-2764144 (all coordinates are in Dm3 2006 genome release) were PCR amplified from genomic DNA and cloned into the FRT cassette of *yellow-attB-mobile* vector (Schwartz *et al.* 2012) using *Xba*I, *Not*I, *Nhe*I, or *Aor*51HI sites. The sequences of the PCR primers are indicated in Table S1. The resulted transgenic constructs were injected into preblastoderm embryos by BestGene for integration in the ZH-51D landing site using *phi*C31 recombination (Bischof *et al.* 2007). Transgenic constructs carrying 680-bp *gypsy* insulator and five random control fragments were described in Schwartz *et al.* (2012). The transgenes were further mobilized by crossing with the source of *P*-element transposase $y^1\ w^1$; *Ki*^{1} *P[ry[+t7.2]= Delta2-3]99B* (Figure S4). After mobilization new integration events were selected by segregation of the *yellow* reporter gene that marked our constructs and the RFP reporter gene that marked the ZH-51D landing site (Bischof *et al.* 2007). To "excise" the tested DNA fragments from the FRT cassette transgenic flies were crossed to the source of FLP-recombinase $y^1\ w^*$; sna^{Sco}/*CyO, P[ry[+t7.2]=70FLP]*, S^2, and expression of FLP recombinase induced by 2-hr heat-shock treatments (37°) during the first 3 days of larval development.

The rescue of CTCF mutations

The pOneStrepCTCFattB construct to rescue *CTCF* loss of function was assembled by placing the N-terminal One-StrEP-tag (IBA) fused in frame with the 2.6-kb *CTCF* ORF under control of the ubiquitous promoter of the *Ubi-p63E* gene (Butcher *et al.* 2004). The *CTCF* ORF was amplified by PCR from genomic DNA using KAPA HiFi DNA Polymerase (Kapa Biosystems) and the primers 5′ CTCF (5′-ttcgaaaaag**cggccGCG**CCAAGGAGGACAAAAAAGGA-3′, the introduced *Not*I site, and the substitution of ATG-Met to GCG-Ala are highlighted in boldface type) and 3′ CTCF (5′-gctagctggcctc**gaTATC**AGGAGACTAAGAGTCCTGC-3′, the introduced *Eco*RV site is highlighted in boldface type). Correct amplification of the *CTCF* ORF was checked by sequencing. The DNA sequence of the pOneStrepCTCFattB construct and further cloning details are available upon request. The pOneStrepCTCFattB construct was integrated in the ZH-51C landing site via *phi*C31 recombination to yield the following transgenic chromosome *M[3xP3-RFP.* w^{+mC} = *Ubi-OneStrepCTCF]ZH-51C* is hereafter referred to as *RC*. To test the rescue of the lethality and homeotic transformations, the y^1w^1; *RC*/+; TM6B, *Tb*/MKRS, *Sb* flies were crossed with $CTCF^{y+1}$/TM6B, *Tb* flies. From the progeny of this cross, the y^1w^1; *RC*/+; $CTCF^{y+1}$/TM6, *Tb* flies were further crossed with the $CTCF^{P35.2}$/TM6B, *Tb* or $CTCF^{9}$/TM6B, *Tb* flies. Both crosses produced a class of flies lacking the Tb phenotype. Most of the Tb-negative flies had the RC chromosome, identified by RFP expression in the eyes, and showed no homeotic transformation. The rare Tb-negative flies lacking RFP expression, the $CTCF^{y+1}/CTCF^{P35.2}$ or $CTCF^{y+1}/CTCF^{9}$ escapers, all displayed characteristic homeotic transformations of posterior abdominal segments. Stable y^1w^1; *RC*; $CTCF^{y+1}/CTCF^{9}$ and y^1w^1; *RC*; $CTCF^{y+1}/CTCF^{P35.2}$ lines were established. After extensive interbreeding, the y^1w^1; *RC*; $CTCF^{y+1}/CTCF^{9}$ stock was used to segregate the y^1w^1; *RC*; $CTCF^{9}$ flies by tracking the loss of transgenic *yellow* that marks the $CTCF^{y+1}$ allele. The same stock was used to derive y^1w^1; *RC*; $CTCF^{y+1}$ flies by repeated crossing to y^1w^1; $CTCF^{y+1}$/*TM6B*, *Tb* females.

Immunostaining of embryos, larval nerve cords, and pupal epithelia

Primary antibodies used were mouse monoclonal anti-Ubx (Ubx FP3.38, 1:20 dilution, Developmental Studies Hybridoma Bank), goat polyclonal anti-Abd-A (dH-17, 1:50, Santa Cruz Biotechnology, sc-27063), mouse monoclonal anti-Abd-B (1A2E9, 1:10, Developmental Studies Hybridoma Bank) and rabbit anti-GFP (1:50, Abcam). Secondary antibodies were donkey antimouse Alexa Fluor 488, donkey anti-goat Alexa Fluor 555, donkey antirabbit Alexa Fluor 488, goat antirabbit Alexa Fluor 488 (Molecular Probes), and goat antimouse Alexa Fluor 555 (Abcam) used at 1:300 dilution. The immunostaining was done essentially as described by Patel (1994) and Wang and Yoder (2011). To control for immunostaining variability, homozygous (mutant) and heterozygous (control) embryos and larval nerve cords were stained simultaneously

in the same vial. Fluorescent images were acquired with a Leica TCS SPE confocal microscope and the images reconstructed from *Z*-stacks using accompanying software. The images were classified as heterozygous or homozygous for the mutation according to GFP expression from a balancer chromosome and the embryonic developmental stage was determined based on the gut morphology. The stage 16 and stage 17 embryos were compared side by side. The effect of mutations on the embryonic immunostaining was assessed with a blind test. An independent evaluator was presented a set of unmarked pictures and asked to sort them into two groups based on intensity of the Abd-B immunostaining in posterior epidermis. For each blind test, 14–40 embryos were examined. With ~80% accuracy, the *mod(mdg4)^{m9}/mod(mdg4)^{m9}* and *Cp190^{P1} mod(mdg4)^{m9}/Cp190^{P1} mod(mdg4)^{m9}* mutant embryos were placed in the low staining group.

Preparation of adult fly cuticles

Adult or pharate adult flies were collected and boiled for 8–10 min in 10% KOH, washed with 1× PBS, dehydrated with 70% and 95% ethanol and stored in 100% glycerol. The cuticles were mounted on microscope slides and photographed with a Nikon SMZ1500 stereomicroscope equipped with DS-Fi1 digital camera.

Fly stocks and genetic analyses

Flies were maintained at 25° on the standard medium. The *CP190^{3}*, *CP190^{EN15}*, *CP190^{P1}*, *CTCF^{9}*, *CTCF$^{P35.2}$* *CTCF^{y+1}*, *CTCF^{GE24185}*, *mod(mdg4)^{u1}*, *mod(mdg4)^{neo129}*, *Fub*, and *Su(Hw)^{v},P[w+,RpII15]/su(Hw)^{f},Ubx* mutant stocks were generously provided by C. Y. Pai, J. W. Raff, K. A. Maggert, V. G. Corces, R. Renkawitz, R. Dorn, W. Bender, P. G. Georgiev, and D. Dorsett. The *CTCF^{EY15833}* flies were obtained from the Bloomington *Drosophila* Stock Center (BDSC, 21162) and *mod(mdg4)^{GS23019}* from the Kyoto *Drosophila* Genetic Resource Center (DGRC, 204647). The *w^{1118}*; *P[RS3]mod(mdg4)$^{CB-6686-3}$* and *w^{1118}*; *P[RS5]mod(mdg4)$^{5-HA-1224}$* stocks (DGRC, 124182 and 125151) were used to generate the *mod(mdg4)^{m9}* deficiency.

The *CTCF^{y+1}* allele was generated by imprecise excision of the P[EPgy2]CTCF^{EY15833} transposon but was not fully characterized (Gerasimova *et al.* 2007). To map the deletion breakpoints, the junction between the remaining part the transgenic *white* reporter gene and the adjacent genomic DNA was PCR amplified using the qm-fw1 and white-fw3 primers and the PCR product sequenced (Figure S1A, Table S2). The unpublished *CTCF^{9}* allele generated in the laboratory of K. A. Maggert was not molecularly characterized. To partially characterize the *CTCF^{9}* molecular lesion, the DNA from *CTCF^{9}/CTCF^{y+1}* early pupa was extracted and analyzed by PCR with the following primer sets: CTCFrev1/CTCFfw2, CTCFrev3/CTCFfw3, CTCFrev2/CTCFfw4, and CTCFrev4/CTCFfw5 (Table S2). This analysis indicates that the *CTCF^{9}* allele is a deletion that removes a region that extends at least between positions 7347182 and 7348943 of chromosome 3R (Figure 1B, Figure S1B).

Molecular structure of the *mod(mdg4)^{m9}* allele was confirmed by partial sequencing of the 5.7-kb PCR product amplified with Long PCR Enzyme Mix (Thermo Scientific) and mod-fw2 and mod-rev primers (Table S2). We note that the *mod(mdg4)^{m9}* chromosome still contains two FRT sites and 3′ part of *mini-white* between them (Figure S1C). The third chromosome of the original *mod(mdg4)^{GS23019}* fly stock (DGRC, 204647) carried unrelated lethal mutation. Segregating this mutation by recombination with wild-type chromosomes revealed that flies homozygous for the *mod(mdg4)^{GS23019}* allele are viable. The *mod(mdg4)^{GS23019}* allele results from the insertion of the *P[GSV7]* transposon (Toba *et al.* 1999) in the beginning of the open reading frame within the second exon of the *mod(mdg4)* gene (Figure 1D). PCR with p395 and modLrev primers (Table S2) and sequencing of the PCR product revealed orientation of the *P[GSV7]* insertion and showed that the ATG sequence of the 5′ *P*-element end from the *P[GSV7]* transposon restores the open reading frame of the *mod(mdg4)* gene with loss of only the first eight amino acids (Figure S1D). We hypothesize that in the absence of GAL4 the *UAS-hsp* promoter of the *P[GSV7]* transposon drives low level expression of the restored *mod(mdg4)* open reading frame and leads to production of some functional protein. Consistent with this hypothesis, adding the ubiquitous source of GAL4 (*y^{1} w**; *P[w^{+mC} Act5C-GAL4]17bFO1/TM6B*, *Tb^{1}* from BDSC, 3954), which enhances the expression from the *UAS-hsp* promoter, rescues the lethality and suppresses homeotic transformations of *mod(mdg4)^{GS23019}/mod(mdg4)^{m9}* flies.

To assess the effects of mutations on female fertility, the same number (20–30) of homozygous or heterozygous females were mated with 10–15 heterozygous males. The females were deemed to have reduced fertility if the cross yielded much fewer progeny (fivefold or greater reduction) than the heterozygous control. To assess the lethality stage, chromosomes carrying mutant alleles were balanced over TM6B marked with *Tb*. Progression of animals homozygous for a mutation was monitored following the Tb phenotype. Stages of pupal lethality were defined according to (Bainbridge and Bownes (1981). Mutations that arrested development at stages P1–P4 were classified as early pupal lethality; those that stopped development at stages P12–P15 were designated as late pupal lethality. When mutants died at pharate adult stage all adult structures were formed and the animals often tried to escape the pupal case but died during the process. No fewer than 100 mutant flies were examined to determine a lethal stage. To describe quantitative characteristics of homeotic transformations 20–50 mutant males and females were examined. In cases of pharate adult lethality, these were often extracted from pupal cases.

Enhancer-blocking assay

Pigmentation of wing blades and abdominal stripes of the body cuticle was scored in 3-day-old females by using a five-grade pigmentation scale (Morris *et al.* 1998), with pigmentation scores of 1 and 5 corresponding to null and wild-type

phenotypes, respectively. To document phenotypes, flies were photographed using a Nikon SMZ1500 stereomicroscope and DS-Fi1 digital camera.

Computational analyses

Normalized ultrahigh-coverage Hi-C data (Schuettengruber *et al.* 2014) were downloaded from Gene Expression Omnibus (GEO) (accession no. GSE61471). The square matrix of contact frequencies between 5000-bp fragments covering the bithorax complex was constructed using custom Perl script and the contact frequencies were plotted with heatmap.2 and colorRampPalette functions from the gplots and RColorBrewer R packages.

The CTCF, Cp190, Su(Hw), and Mod(mdg4)67.2 genomic binding profiles (ChIP/input ratios) were from Schwartz *et al.* (2012). The genomic binding profile (read density) of all Mod(mdg4) isoforms was derived from ChIP-seq mapping by Van Bortle *et al.* (2012). Briefly, fastq files were downloaded from GEO (accession no. GSM892322) and reads aligned to the Dm3 2006 *Drosophila melanogaster* reference genome with bowtie2 (Langmead and Salzberg 2012) using default parameters. The reads were further tested for strand correlation, extended accordingly, and read density profiles generated using Pyicos (Althammer *et al.* 2011).

Acknowledgments

We are grateful to C. Y. Pai, J. W. Raff, K. A. Maggert, V. G. Corces, R. Renkawitz, R. Dorn, W. Bender, P. G. Georgiev, and D. Dorsett for generous gifts of fly stocks. We thank Giacomo Cavalli and Jia-Ming Chang for suggesting that *Fub* is a topological boundary. We are grateful to Per Stenberg for help with processing of the Hi-C data and Fredrik Hugosson, Yasuo Yamazaki, and Georg Wolfstetter for advice on confocal microscopy. We thank Allison Churcher, François Karch, Pamela Geyer, and an anonymous reviewer for critical comments on the manuscript. This work was supported in part by grants from the European Network of Excellence EpiGeneSys, Kempestiftelserna, Erik Philip-Sörensen Stiftelse, Carl Tryggers Stiftelse to Y.B.S. and Knut och Alice Wallenbergs Stiftelse to EpiCoN (Y.B.S., co-principal investigator). Stocks obtained from the Bloomington *Drosophila* Stock Center [National Institutes of Health (NIH) P40OD018537] and the Kyoto *Drosophila* Genetic Resource Center were used in this study. The Ubx FP3.38 and Abd-B 1A2E9 monoclonal antibodies were obtained from the Developmental Studies Hybridoma Bank, created by the National Institute of Child Health and Human Development of the NIH and maintained at the Department of Biology, University of Iowa, Iowa City, IA 52242.

Literature Cited

Althammer, S., J. Gonzalez-Vallinas, C. Ballare, M. Beato, and E. Eyras, 2011 Pyicos: a versatile toolkit for the analysis of high-throughput sequencing data. Bioinformatics 27: 3333–3340.

Aoki, T., A. Sarkeshik, J. Yates, and P. Schedl, 2012 Elba, a novel developmentally regulated chromatin boundary factor is a hetero-tripartite DNA binding complex. eLife 1: e00171.

Bainbridge, S. P., and M. Bownes, 1981 Staging the metamorphosis of Drosophila melanogaster. J. Embryol. Exp. Morphol. 66: 57–80.

Baniahmad, A., C. Steiner, A. C. Kohne, and R. Renkawitz, 1990 Modular structure of a chicken lysozyme silencer: involvement of an unusual thyroid hormone receptor binding site. Cell 61: 505–514.

Barges, S., J. Mihaly, M. Galloni, K. Hagstrom, M. Muller *et al.*, 2000 The Fab-8 boundary defines the distal limit of the bithorax complex iab-7 domain and insulates iab-7 from initiation elements and a PRE in the adjacent iab-8 domain. Development 127: 779–790.

Bender, W., and M. Lucas, 2013 The border between the ultrabithorax and abdominal-A regulatory domains in the *Drosophila* bithorax complex. Genetics 193: 1135–1147.

Bischof, J., R. K. Maeda, M. Hediger, F. Karch, and K. Basler, 2007 An optimized transgenesis system for Drosophila using germ-line-specific phiC31 integrases. Proc. Natl. Acad. Sci. USA 104: 3312–3317.

Bonchuk, A., S. Denisov, P. Georgiev, and O. Maksimenko, 2011 Drosophila BTB/POZ domains of "ttk group" can form multimers and selectively interact with each other. J. Mol. Biol. 412: 423–436.

Bonchuk, A., O. Maksimenko, O. Kyrchanova, T. Ivlieva, V. Mogila *et al.*, 2015 Functional role of dimerization and CP190 interacting domains of CTCF protein in Drosophila melanogaster. BMC Biol. 13: 63.

Buchner, K., P. Roth, G. Schotta, V. Krauss, H. Saumweber *et al.*, 2000 Genetic and molecular complexity of the position effect variegation modifier mod(mdg4) in Drosophila. Genetics 155: 141–157.

Butcher, R. D., S. Chodagam, R. Basto, J. G. Wakefield, D. S. Henderson *et al.*, 2004 The Drosophila centrosome-associated protein CP190 is essential for viability but not for cell division. J. Cell Sci. 117: 1191–1199.

Cleard, F., Y. Moshkin, F. Karch, and R. K. Maeda, 2006 Probing long-distance regulatory interactions in the Drosophila melanogaster bithorax complex using Dam identification. Nat. Genet. 38: 931–935.

Cuartero, S., U. Fresan, O. Reina, E. Planet, and M. L. Espinas, 2014 Ibf1 and Ibf2 are novel CP190-interacting proteins required for insulator function. EMBO J. 33: 637–647.

Dorn, R., V. Krauss, G. Reuter, and H. Saumweber, 1993 The enhancer of position-effect variegation of Drosophila, E(var)3–93D, codes for a chromatin protein containing a conserved domain common to several transcriptional regulators. Proc. Natl. Acad. Sci. USA 90: 11376–11380.

Dorn, R., G. Reuter, and A. Loewendorf, 2001 Transgene analysis proves mRNA trans-splicing at the complex mod(mdg4) locus in Drosophila. Proc. Natl. Acad. Sci. USA 98: 9724–9729.

Galloni, M., H. Gyurkovics, P. Schedl, and F. Karch, 1993 The bluetail transposon: evidence for independent cis-regulatory domains and domain boundaries in the bithorax complex. EMBO J. 12: 1087–1097.

Gaszner, M., J. Vazquez, and P. Schedl, 1999 The Zw5 protein, a component of the scs chromatin domain boundary, is able to block enhancer-promoter interaction. Genes Dev. 13: 2098–2107.

Gause, M., P. Morcillo, and D. Dorsett, 2001 Insulation of enhancer-promoter communication by a gypsy transposon insert in the Drosophila cut gene: cooperation between suppressor of hairy-wing and modifier of mdg4 proteins. Mol. Cell. Biol. 21: 4807–4817.

Georgiev, P., and M. Kozycina, 1996 Interaction between mutations in the suppressor of Hairy wing and modifier of mdg4 genes of Drosophila melanogaster affecting the phenotype of gypsy-induced mutations. Genetics 142: 425–436.

Georgiev, P. G., and T. I. Gerasimova, 1989 Novel genes influencing the expression of the yellow locus and mdg4 (gypsy) in Drosophila melanogaster. Mol. Gen. Genet. 220: 121–126.

Gerasimova, T. I., and V. G. Corces, 1998 Polycomb and trithorax group proteins mediate the function of a chromatin insulator. Cell 92: 511–521.
Gerasimova, T. I., D. A. Gdula, D. V. Gerasimov, O. Simonova, and V. G. Corces, 1995 A Drosophila protein that imparts directionality on a chromatin insulator is an enhancer of position-effect variegation. Cell 82: 587–597.
Gerasimova, T. I., E. P. Lei, A. M. Bushey, and V. G. Corces, 2007 Coordinated control of dCTCF and gypsy chromatin insulators in Drosophila. Mol. Cell 28: 761–772.
Geyer, P. K., and V. G. Corces, 1992 DNA position-specific repression of transcription by a Drosophila zinc finger protein. Genes Dev. 6: 1865–1873.
Golic, K. G., and M. M. Golic, 1996 Engineering the Drosophila genome: chromosome rearrangements by design. Genetics 144: 1693–1711.
Golovnin, A., I. Biryukova, O. Romanova, M. Silicheva, A. Parshikov *et al.*, 2003 An endogenous Su(Hw) insulator separates the yellow gene from the Achaete-scute gene complex in Drosophila. Development 130: 3249–3258.
Golovnin, A., A. Mazur, M. Kopantseva, M. Kurshakova, P. V. Gulak *et al.*, 2007 Integrity of the Mod(mdg4)-67.2 BTB domain is critical to insulator function in Drosophila melanogaster. Mol. Cell. Biol. 27: 963–974.
Gruzdeva, N., O. Kyrchanova, A. Parshikov, A. Kullyev, and P. Georgiev, 2005 The Mcp element from the bithorax complex contains an insulator that is capable of pairwise interactions and can facilitate enhancer-promoter communication. Mol. Cell. Biol. 25: 3682–3689.
Hagstrom, K., M. Muller, and P. Schedl, 1996 Fab-7 functions as a chromatin domain boundary to ensure proper segment specification by the Drosophila bithorax complex. Genes Dev. 10: 3202–3215.
Iampietro, C., F. Cleard, H. Gyurkovics, R. K. Maeda, and F. Karch, 2008 Boundary swapping in the Drosophila Bithorax complex. Development 135: 3983–3987.
Karch, F., 2015 In vivo studies of the Drosophila insulator factor CTCF reach a Catch 22. BMC Biol. 13: 71.
Karch, F., W. Bender, and B. Weiffenbach, 1990 abdA expression in Drosophila embryos. Genes Dev. 4: 1573–1587.
Karch, F., M. Galloni, L. Sipos, J. Gausz, H. Gyurkovics *et al.*, 1994 Mcp and Fab-7: molecular analysis of putative boundaries of cis-regulatory domains in the bithorax complex of Drosophila melanogaster. Nucleic Acids Res. 22: 3138–3146.
Kuhn-Parnell, E. J., C. Helou, D. J. Marion, B. L. Gilmore, T. J. Parnell *et al.*, 2008 Investigation of the properties of non-gypsy suppressor of hairy-wing-binding sites. Genetics 179: 1263–1273.
Langmead, B., and S. L. Salzberg, 2012 Fast gapped-read alignment with Bowtie 2. Nat. Methods 9: 357–359.
Lanzuolo, C., V. Roure, J. Dekker, F. Bantignies, and V. Orlando, 2007 Polycomb response elements mediate the formation of chromosome higher-order structures in the bithorax complex. Nat. Cell Biol. 9: 1167–1174.
Le Gall, A., A. Valeri, and M. Nollmann, 2015 Roles of chromatin insulators in the formation of long-range contacts. Nucleus 6: 118–122.
Li, H. B., M. Muller, I. A. Bahechar, O. Kyrchanova, K. Ohno *et al.*, 2011 Insulators, not Polycomb response elements, are required for long-range interactions between Polycomb targets in Drosophila melanogaster. Mol. Cell. Biol. 31: 616–625.
Ling, J. Q., T. Li, J. F. Hu, T. H. Vu, H. L. Chen *et al.*, 2006 CTCF mediates interchromosomal colocalization between Igf2/H19 and Wsb1/Nf1. Science 312: 269–272.
Lobanenkov, V. V., R. H. Nicolas, V. V. Adler, H. Paterson, E. M. Klenova *et al.*, 1990 A novel sequence-specific DNA binding protein which interacts with three regularly spaced direct repeats of the CCCTC-motif in the 5′-flanking sequence of the chicken c-myc gene. Oncogene 5: 1743–1753.
Macias, A., J. Casanova, and G. Morata, 1990 Expression and regulation of the abd-A gene of Drosophila. Development 110: 1197–1207.
Maeda, R. K., and F. Karch, 2006 The ABC of the BX-C: the bithorax complex explained. Development 133: 1413–1422.
Maksimenko, O., M. Bartkuhn, V. Stakhov, M. Herold, N. Zolotarev *et al.*, 2015 Two new insulator proteins, Pita and ZIPIC, target CP190 to chromatin. Genome Res. 25: 89–99.
Matzat, L. H., R. K. Dale, N. Moshkovich, and E. P. Lei, 2012 Tissue-specific regulation of chromatin insulator function. PLoS Genet. 8: e1003069.
Matzat, L. H., and E. P. Lei, 2014 Surviving an identity crisis: a revised view of chromatin insulators in the genomics era. Biochim. Biophys. Acta 1839: 203–214.
Mihaly, J., I. Hogga, J. Gausz, H. Gyurkovics, and F. Karch, 1997 In situ dissection of the Fab-7 region of the bithorax complex into a chromatin domain boundary and a Polycomb-response element. Development 124: 1809–1820.
Mohan, M., M. Bartkuhn, M. Herold, A. Philippen, N. Heinl *et al.*, 2007 The Drosophila insulator proteins CTCF and CP190 link enhancer blocking to body patterning. EMBO J. 26: 4203–4214.
Moon, H., G. Filippova, D. Loukinov, E. Pugacheva, Q. Chen *et al.*, 2005 CTCF is conserved from Drosophila to humans and confers enhancer blocking of the Fab-8 insulator. EMBO Rep. 6: 165–170.
Morris, J. R., J. L. Chen, P. K. Geyer, and C. T. Wu, 1998 Two modes of transvection: enhancer action in trans and bypass of a chromatin insulator in cis. Proc. Natl. Acad. Sci. USA 95: 10740–10745.
Negre, N., C. D. Brown, P. K. Shah, P. Kheradpour, C. A. Morrison *et al.*, 2010 A comprehensive map of insulator elements for the Drosophila genome. PLoS Genet. 6: e1000814.
Negre, N., C. D. Brown, L. Ma, C. A. Bristow, S. W. Miller *et al.*, 2011 A cis-regulatory map of the Drosophila genome. Nature 471: 527–531.
Oliver, D., B. Sheehan, H. South, O. Akbari, and C. Y. Pai, 2010 The chromosomal association/dissociation of the chromatin insulator protein Cp190 of Drosophila melanogaster is mediated by the BTB/POZ domain and two acidic regions. BMC Cell Biol. 11: 101.
Ong, C. T., and V. G. Corces, 2014 CTCF: an architectural protein bridging genome topology and function. Nat. Rev. Genet. 15: 234–246.
Pai, C. Y., E. P. Lei, D. Ghosh, and V. G. Corces, 2004 The centrosomal protein CP190 is a component of the gypsy chromatin insulator. Mol. Cell 16: 737–748.
Parnell, T. J., M. M. Viering, A. Skjesol, C. Helou, E. J. Kuhn *et al.*, 2003 An endogenous suppressor of hairy-wing insulator separates regulatory domains in Drosophila. Proc. Natl. Acad. Sci. USA 100: 13436–13441.
Parnell, T. J., E. J. Kuhn, B. L. Gilmore, C. Helou, M. S. Wold *et al.*, 2006 Identification of genomic sites that bind the Drosophila suppressor of Hairy-wing insulator protein. Mol. Cell. Biol. 26: 5983–5993.
Patel, N. H., 1994 Imaging neuronal subsets and other cell types in whole-mount Drosophila embryos and larvae using antibody probes. Methods Cell Biol. 44: 445–487.
Ramos, E., D. Ghosh, E. Baxter, and V. G. Corces, 2006 Genomic organization of gypsy chromatin insulators in *Drosophila melanogaster*. Genetics 172: 2337–2349.
Rao, S. S., M. H. Huntley, N. C. Durand, E. K. Stamenova, I. D. Bochkov *et al.*, 2014 A 3D map of the human genome at kilobase resolution reveals principles of chromatin looping. Cell 159: 1665–1680.
Rodin, S., O. Kyrchanova, E. Pomerantseva, A. Parshikov, and P. Georgiev, 2007 New properties of Drosophila fab-7 insulator. Genetics 177: 113–121.

Ryder, E., F. Blows, M. Ashburner, R. Bautista-Llacer, D. Coulson *et al.*, 2004 The DrosDel collection: a set of P-element insertions for generating custom chromosomal aberrations in *Drosophila melanogaster*. Genetics 167: 797–813.

Schuettengruber, B., N. Oded Elkayam, T. Sexton, M. Entrevan, S. Stern *et al.*, 2014 Cooperativity, specificity, and evolutionary stability of Polycomb targeting in Drosophila. Cell Reports 9: 219–233.

Schwartz, Y. B., D. Linder-Basso, P. V. Kharchenko, M. Y. Tolstorukov, M. Kim *et al.*, 2012 Nature and function of insulator protein binding sites in the Drosophila genome. Genome Res. 22: 2188–2198.

Schweinsberg, S., K. Hagstrom, D. Gohl, P. Schedl, R. P. Kumar *et al.*, 2004 The enhancer-blocking activity of the Fab-7 boundary from the Drosophila bithorax complex requires GAGA-factor-binding sites. Genetics 168: 1371–1384.

Sexton, T., E. Yaffe, E. Kenigsberg, F. Bantignies, B. Leblanc *et al.*, 2012 Three-dimensional folding and functional organization principles of the Drosophila genome. Cell 148: 458–472.

Singh, N. P., and R. K. Mishra, 2014 Role of abd-A and Abd-B in development of abdominal epithelia breaks posterior prevalence rule. PLoS Genet. 10: e1004717.

Soltani-Bejnood, M., S. E. Thomas, L. Villeneuve, K. Schwartz, C. S. Hong *et al.*, 2007 Role of the mod(mdg4) common region in homolog segregation in Drosophila male meiosis. Genetics 176: 161–180.

Soshnev, A. A., R. M. Baxley, J. R. Manak, K. Tan, and P. K. Geyer, 2013 The insulator protein Suppressor of Hairy-wing is an essential transcriptional repressor in the Drosophila ovary. Development 140: 3613–3623.

Spana, C., D. A. Harrison, and V. G. Corces, 1988 The Drosophila melanogaster suppressor of Hairy-wing protein binds to specific sequences of the gypsy retrotransposon. Genes Dev. 2: 1414–1423.

Splinter, E., H. Heath, J. Kooren, R. J. Palstra, P. Klous *et al.*, 2006 CTCF mediates long-range chromatin looping and local histone modification in the beta-globin locus. Genes Dev. 20: 2349–2354.

Spradling, A. C., and G. M. Rubin, 1982 Transposition of cloned P elements into Drosophila germ line chromosomes. Science 218: 341–347.

Struhl, G., and R. A. White, 1985 Regulation of the Ultrabithorax gene of Drosophila by other bithorax complex genes. Cell 43: 507–519.

Toba, G., T. Ohsako, N. Miyata, T. Ohtsuka, K. H. Seong *et al.*, 1999 The gene search system. A method for efficient detection and rapid molecular identification of genes in *Drosophila melanogaster*. Genetics 151: 725–737.

Van Bortle, K., and V. G. Corces, 2012 Nuclear organization and genome function. Annu. Rev. Cell Dev. Biol. 28: 163–187.

Van Bortle, K., E. Ramos, N. Takenaka, J. Yang, J. E. Wahi *et al.*, 2012 Drosophila CTCF tandemly aligns with other insulator proteins at the borders of H3K27me3 domains. Genome Res. 22: 2176–2187.

Vogelmann, J., A. Le Gall, S. Dejardin, F. Allemand, A. Gamot *et al.*, 2014 Chromatin insulator factors involved in long-range DNA interactions and their role in the folding of the Drosophila genome. PLoS Genet. 10: e1004544.

Wang, W., and J. H. Yoder, 2011 Drosophila pupal abdomen immunohistochemistry. J. Vis. Exp. 56: e3139 doi: 10.3791/3139.

Wolle, D., F. Cleard, T. Aoki, G. Deshpande, P. Schedl *et al.*, 2015 Functional requirements for Fab-7 boundary activity in the Bithorax Complex. Mol. Cell. Biol. **35:** 3739–3752.

Zhao, K., C. M. Hart, and U. K. Laemmli, 1995 Visualization of chromosomal domains with boundary element-associated factor BEAF-32. Cell 81: 879–889.

Zhou, J., S. Barolo, P. Szymanski, and M. Levine, 1996 The Fab-7 element of the bithorax complex attenuates enhancer-promoter interactions in the Drosophila embryo. Genes Dev. 10: 3195–3201.

Communicating editor: P. Geyer

GENETICS

Supporting Information
www.genetics.org/lookup/suppl/doi:10.1534/genetics.115.179309/-/DC1

Distinct Roles of Chromatin Insulator Proteins in Control of the *Drosophila* Bithorax Complex

Mikhail Savitsky, Maria Kim, Oksana Kravchuk, and Yuri B. Schwartz

DOI: 10.1534/genetics.115.179309

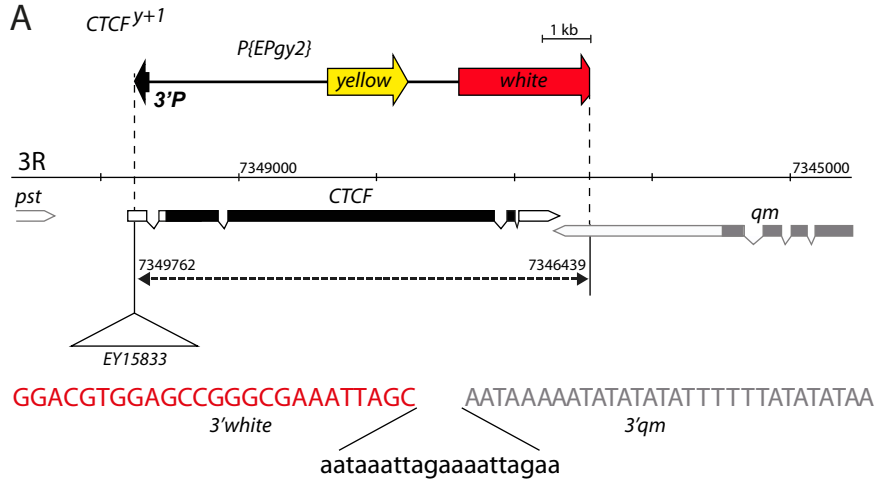

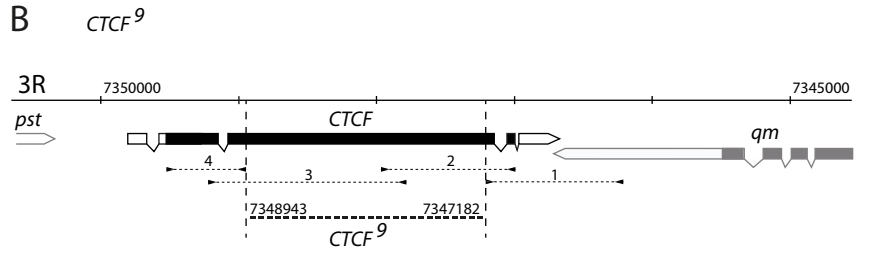

amplicons with primer sets
1. CTCFrev4 / CTCFfw5
2. CTCFrev2 / CTCFfw4
3. CTCFrev3 / CTCFfw3
4. CTCFrev1 / CTCFfw2

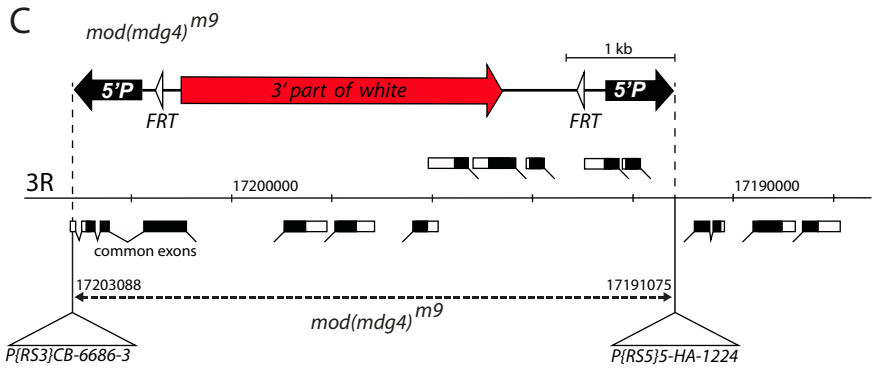

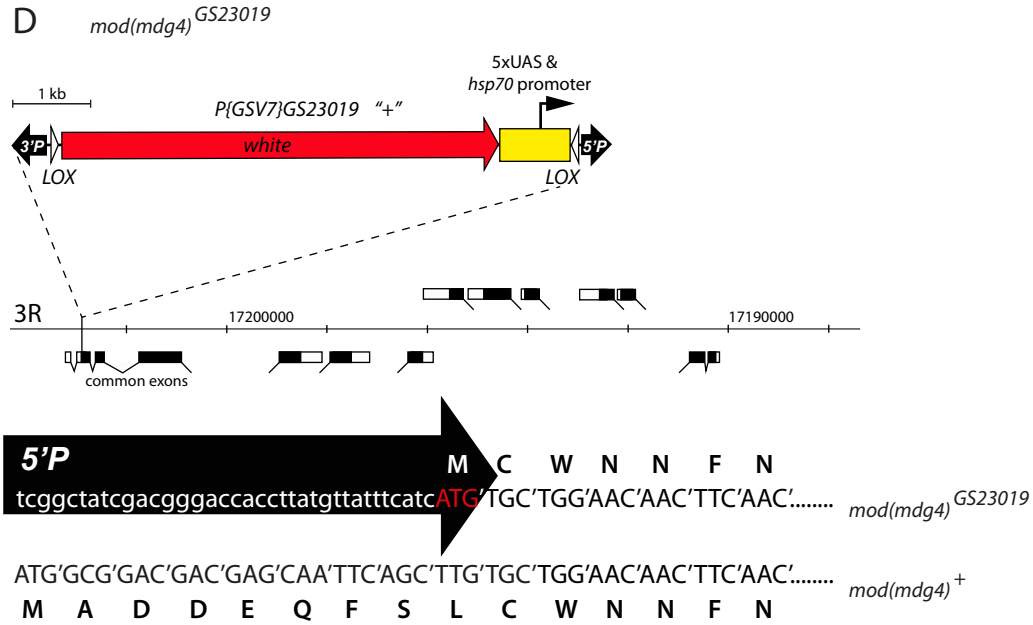

Figure S1. Structures of the *CTCF^{y+1}*, *CTCF^{9}* , *mod(mdg4)^{m9}* and *mod(mdg4)^{GS23019}* alleles. A. The *CTCF^{y+1}* allele is a 3.3kb deletion induced by mobilization of the *P[EPgy]CTCF^{EY15833}* transposon (GERASIMOVA *et al.* 2007). It still contains large portion of the *P[EPgy]CTCF^{EY15833}* transposon with functional *yellow* gene and nonfunctional *white* gene. The deletion removes the 3' part of the *white* gene and the 5' P-element end of the transposon, the entire *CTCF* gene and a small part of the 3' UTR of the adjacent *qm* gene. Shown below is the sequence of the junction between the deletion breakpoints. In addition to the DNA sequences of the *qm* 3' UTR (grey) and the 3' end of the *white* gene (red) it includes 20 nucleotides of an unknown origin. **B.** The extent of the *CTCF^{9}* deletion was partially mapped by PCR with amplicons indicated to the right. None of the amplicons give a product in PCR with genomic DNA of *CTCF^{y+1}* / *CTCF^{9}* flies. This indicates that at least 1.7kb from the central part of the CTCF gene is removed by *CTCF^{9}*. However, the exact breakpoints of the *CTCF^{9}* deletion are unknown. **C.** The *mod(mdg4)^{m9}* deletion was induced by FRT recombination. It still contains portions of the *P[RS5]5-HA-1224* and *P[RS3]CB-6686-3* transposons. The left 5' P-element end and the 3'part of the *white* gene are from the *P[RS5]5-HA-1224* transposon and the right 5' P-element end is from the *P[RS3]CB-6686-3* transposon. **D.** The molecular structure of the *mod(mdg4)^{GS23019}* allele. Note that the ATG sequence of the 5' P-element end from the *P[GSV7]* transposon (black arrow) restores the open reading frame of the *mod(mdg4)* gene with loss of the first 8 amino acids (shown with one letter code). The *UAS-hsp70* promoter of the *P[GSV7]* transposon may drive expression of the resulted synthetic *mod(mdg4)* open reading frame.

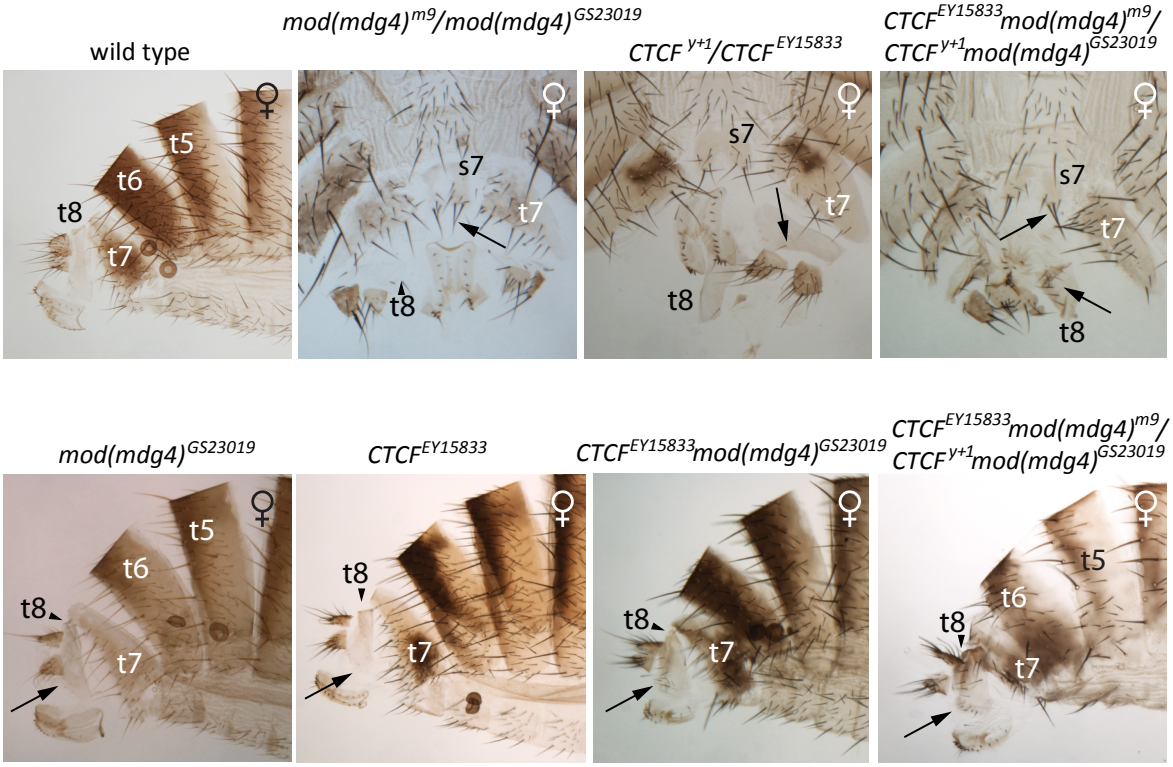

Figure S2. Additional evidence of genetic interactions between the *CTCF* and *mod(mdg4)* alleles. Shown are cuticles of female flies of indicated genotypes. Note much stronger homeotic transformation of segments A7 and A8 in the $CTCF^{y+1}$ $mod(mdg4)^{GS23019}$/ $CTCF^{EY15833}$ $mod(mdg4)^{m9}$ mutants compared to flies with individual mutations in *CTCF* or *mod(mdg4)* or a combination of the weaker $CTCF^{EY15833}$ and $mod(mdg4)^{GS23019}$ alleles. Extra bristles are indicated with arrows and the position of the tergite of segment A8 (t8) is marked with an arrowhead.

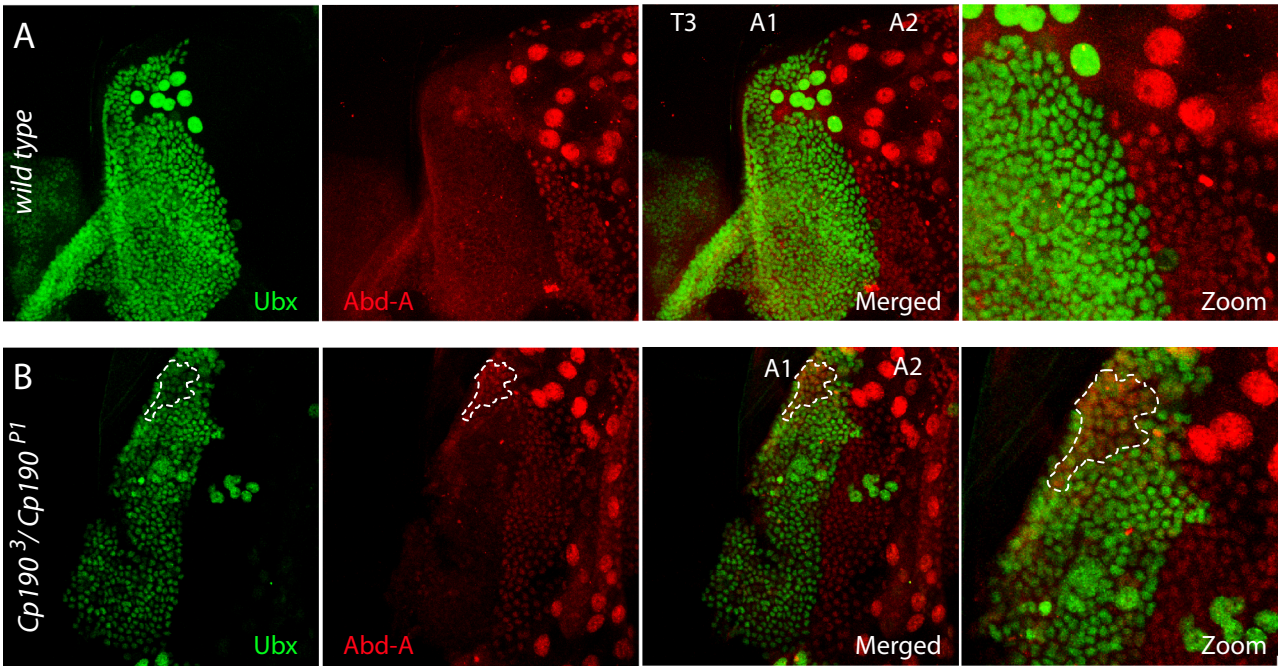

Figure S3. Ectopic expression of the *abd-A* gene in abdominal segment A1 of *Cp190* mutant pupae. The images show corresponding parts of developing adult epithelia (small diploid cells) from wild type (**A**) and $Cp190^{3}/Cp190^{3}$ (**B**) pupae. In wild-type pupae the Abd-A and Ubx - positive cells do not mix and segregate along the A1 - A2 segmental boundary. In *Cp190* mutants the A1 segment has patches of cells (the most obvious marked with white dashed lines) that express Abd-A. The cells that express Abd-A have low Ubx expression. Individual cells are best seen in the blowup (zoom) of the upper right quarters of the merged images.

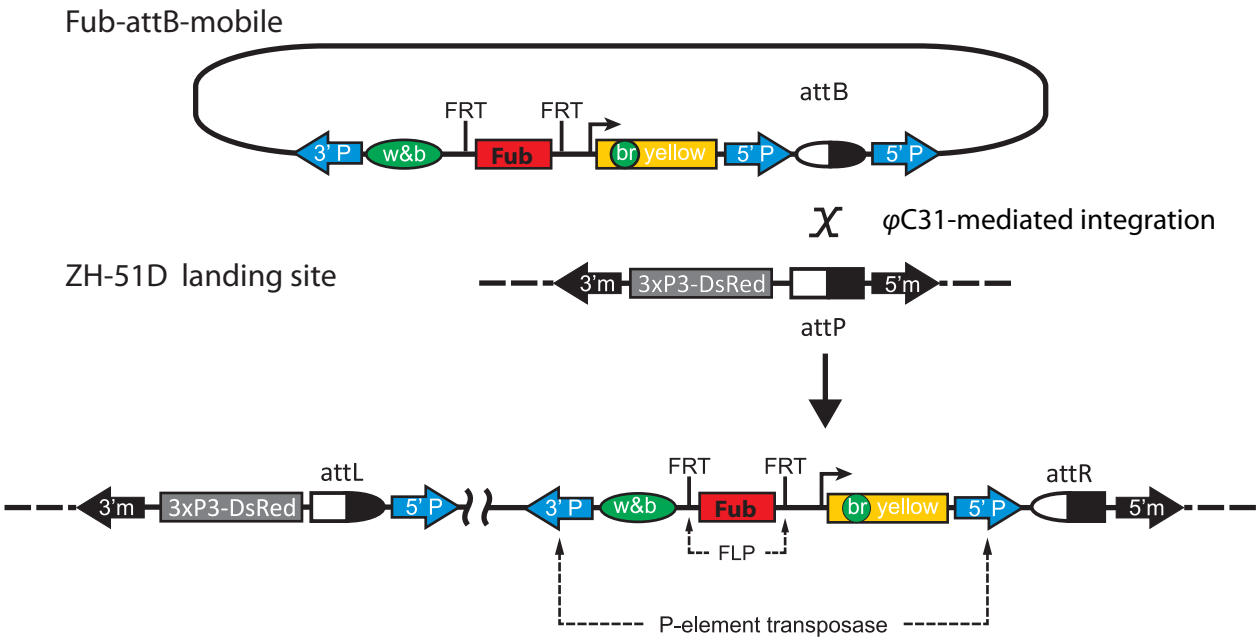

Figure S4. The schematic of the *yellow* enhancer blocking assay. Tested class 12 insulator binding fragments (here exemplified with *Fub* element, red rectangle) are cloned in the FRT cassette placed between the upstream wing and body-specific transcriptional enhancers (green oval) and the promoter of the *yellow* reporter gene. The constructs are integrated in the ZH-51D landing site by ϕC31 mediated recombination for comparison of enhancer-blocking effects within the same chromatin environment and then mobilized by P-element transposition to test how the ability to block is affected by different chromatin environments.

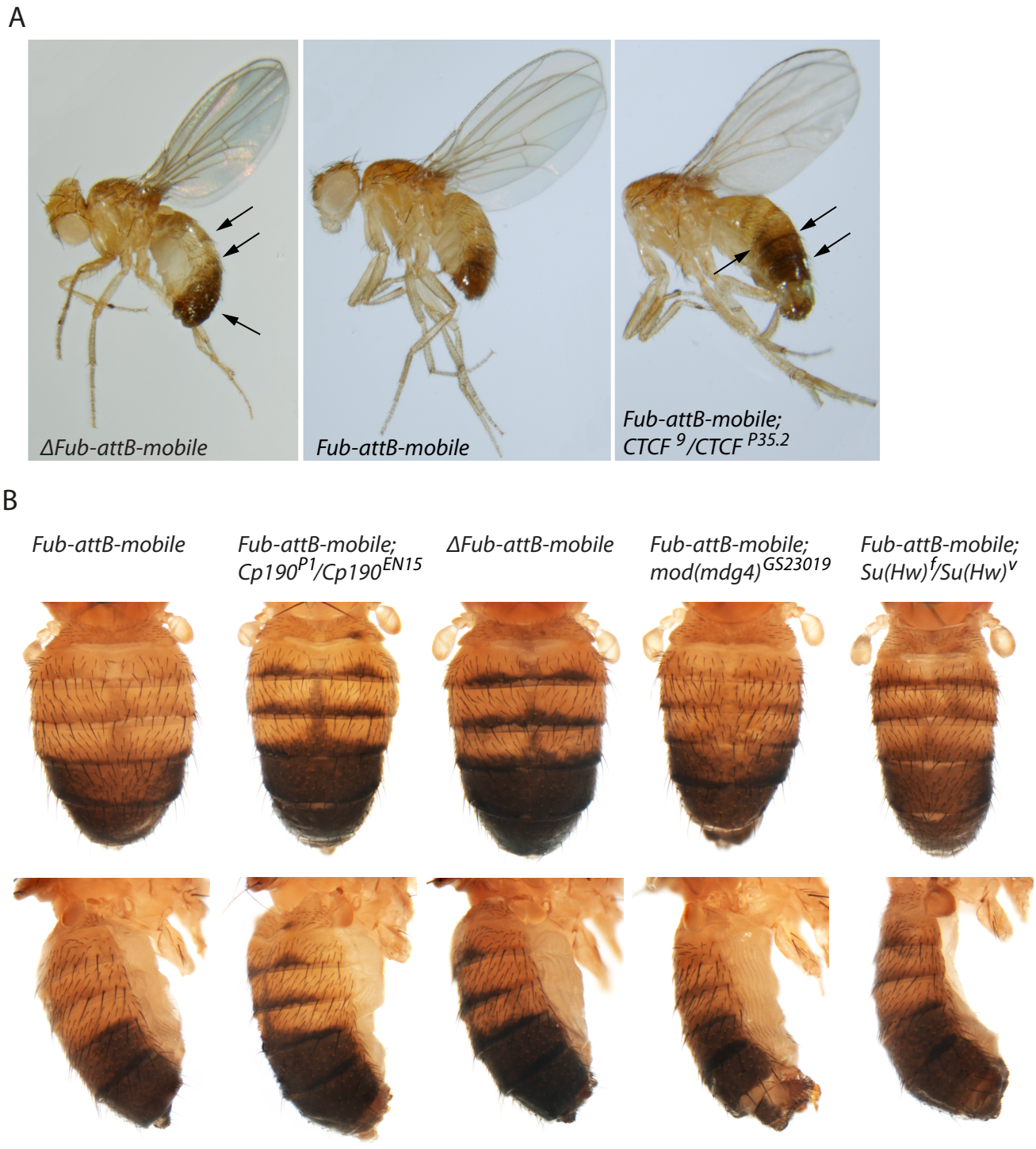

Figure S5. Effects of mutations in different insulator protein coding genes on the enhancer-blocking by *Fub* element. **A.** Loss of *CTCF* function mildly suppresses the enhancer blocking by *Fub*. Arrows indicate stronger pigmentation of abdominal stripes in the *CTCF* mutant flies compared to the *Fub-attB-mobile* flies on wild-type background (center). However, the pigmentation of *CTCF* mutants is notably weaker than that of the *Fub-attB-mobile* flies after *Fub* excision (left). Note that flies photographed for this panel are 2 days old to provide appropriate comparison with $CTCF^{9}/CTCF^{P35.5}$ mutants that die around this stage. This explains the overall lighter color of cuticles and wing blades compared to other images. **B.** Photographs of fly abdomens illustrate that, unlike the excision of the *Fub* element or the mutant *Cp190* background, mutations in *Su(Hw)* and *mod(mdg4*) genes show no effect on the enhancer blocking by *Fub*.

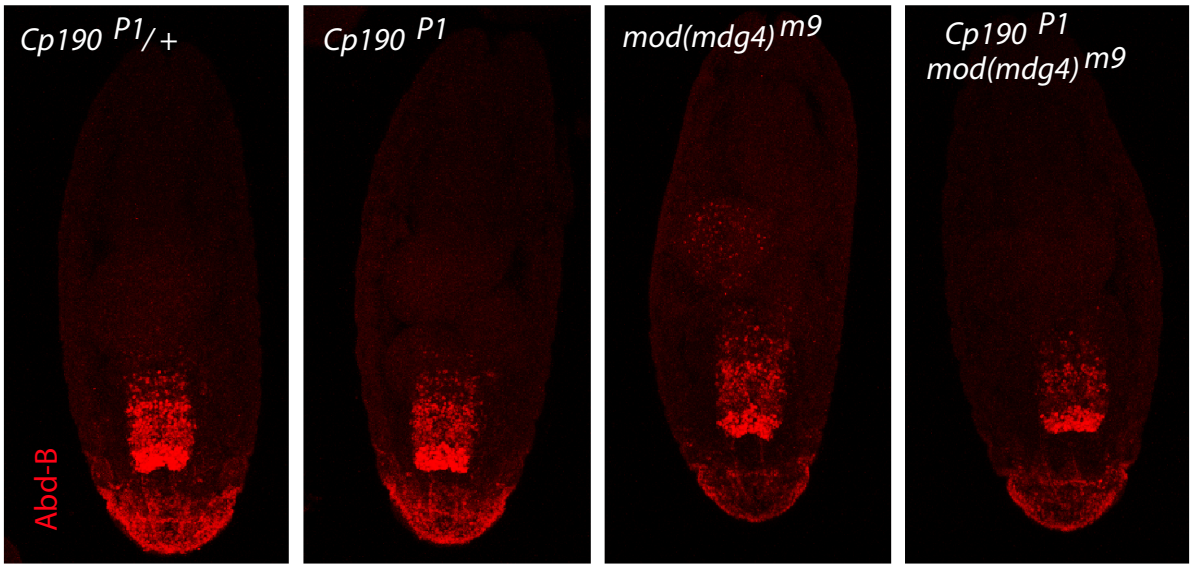

Figure S6. *Cp190* mutation does not do affect the downregulation of *Abd-B* expression in the *mod(mdg4)* mutant embryos. Stage 17 embryos of indicated genotypes were immunostained with antibodies against Abd-B. Representative images indicate that immunostaining of $Cp190^{P1}/Cp190^{P1}$ embryos is no different from that of the matching heterozygous control. The $mod(mdg4)^{m9}/mod(mdg4)^{m9}$ and the $Cp190^{P1}$, $mod(mdg4)^{m9}$/ $Cp190^{P1}$, $mod(mdg4)^{m9}$ embryos display weaker immunostaining of posterior embryonic epidermis compared to heterozygous control, but we see no evidence that the $Cp190^{P1}$ mutation enhances or suppresses the reduction of *Abd-B* expression by $mod(mdg4)^{m9}$.

Table S1. The list of PCR primers for amplification and cloning of Class 12 insulator binding sites into *yellow-attB-mobile* vector.

Fab2fw (XbaI)*	CTTCTCTA**TCTAGA**CCCTAACACTTTTGTGAATCCGTA
Fab2rev (NotI)	CTTCTCTA**GCGGCCGC**AAGTGCACGTTTTGATGAGCTG
12d2-for (XbaI)	ACT**TCTAGA**ATACCCATTACTAGAG
12d2-rev (XbaI)	GCAGAG**TCTAGA**AGTCCAATGTGGA
12d3-for (NheI)	CTTAA**GCTAGC**CACTTGTTTGTAAG
12d3-rev (NheI)	GATAT**GCTAGC**TACTGCCATAACCA
12d4-for (NheI)	CGTC**GCTAGC**ATGACCTTCCACCTTG
12d4-rev (NheI)	TTGC**GCTAGC**CCAGAGCGATCC
12d6-for (Aor51HI)	GTTT**AGCGCT**GGATTCATTAATTTGCC
12d6-rev (Aor51HI)	AGGC**AGCGCT**CGGGGAAACTTTTTT
12r1-for (NheI)	ATTT**GCTAGC**CATTTGATTCTGCTTT
12r1-rev (NheI)	ATC**GCTAGC**GACGTTTTGTGCTCC
12r3-for (NheI)	TGAGT**GCTAGC**TCATGGGATTGC
12r3-rev (NheI)	GACAAGA**GCTAGC**ATGTTTCTATGG
12r4-for (XbaI)	AACT**TCTAGA**ACTCAGACACGCAAAC
12r4-rev (XbaI)	GACAGG**TCTAGA**TATACACAGACGA
12r5-for (NheI)	CGGAT**GCTAGC**AAATCGCTGGAC
12r5-rev (NheI)	AATGG**GCTAGC**ACTGTGGGACGAATG

* the primers contain sites for indicated restriction endonucleases used for cloning

Table S2. The list of PCR primers used for mapping molecular lesions of the mutant alleles.

CTCFfw1	ATAACAAATCCAGCCTGCCCTA
CTCFfw2	ATTACAATTGGTCGTTGCGAGA
CTCFfw3	CGTGGTCAGTACAGCCACCAAT
CTCFfw4	AAGTACCAATGCGACATCTGCAA
CTCFfw5	CAACTCCAAGATCAGTGCCAAAA
CTCFrev1	GTGCCGGTACTTTGACCACTAA
CTCFrev2	CCTGCTCAATCATATCCATCAGCT
CTCFrev3	GCATGTCATTGGCACATCAGAG
CTCFrev4	TTTTAGTTTCGCCCAACGAATG
qm-fw1	TTCAGCTCCAACAAGGAGGAC
qm-fw2	ATAGCGCCAGCATCACGCAGT
qm-rev1	GATCTGGTTCGACTGCGTGAT
y2ex-endfw	CAACAACATAGGGCAACAGCGG
mod-fw2	CAGCAATCTCGTCGCCTGGTA
mod-rev	CGCGAGTCACAGTAGACAAGGAA
modLrev	GGCTGACGTTGTTCAGGAATACT
white-rev3	CCAAAAAGATGAGGCCAATCAAG
white-fw3	AGAAAGGAAGCGTCTGGCATTC
p395 (*P-element*)	TCCGCACACAACCTTTCCTCTCAAC
p394 (*P-element*)	CGCTGTCTCACTCAGACTCAATACGAC